ChemPubSoc Europe
DOI: 10.1002/cphc.201701175
CHEMPHYSCHEM Reviews

Controlling the Outgrowth and Functions of Neural Stem Cells: The Effect of Surface Topography

C. Simitzi,* K. Karali, A. Ranella, and E. Stratakis*[a]

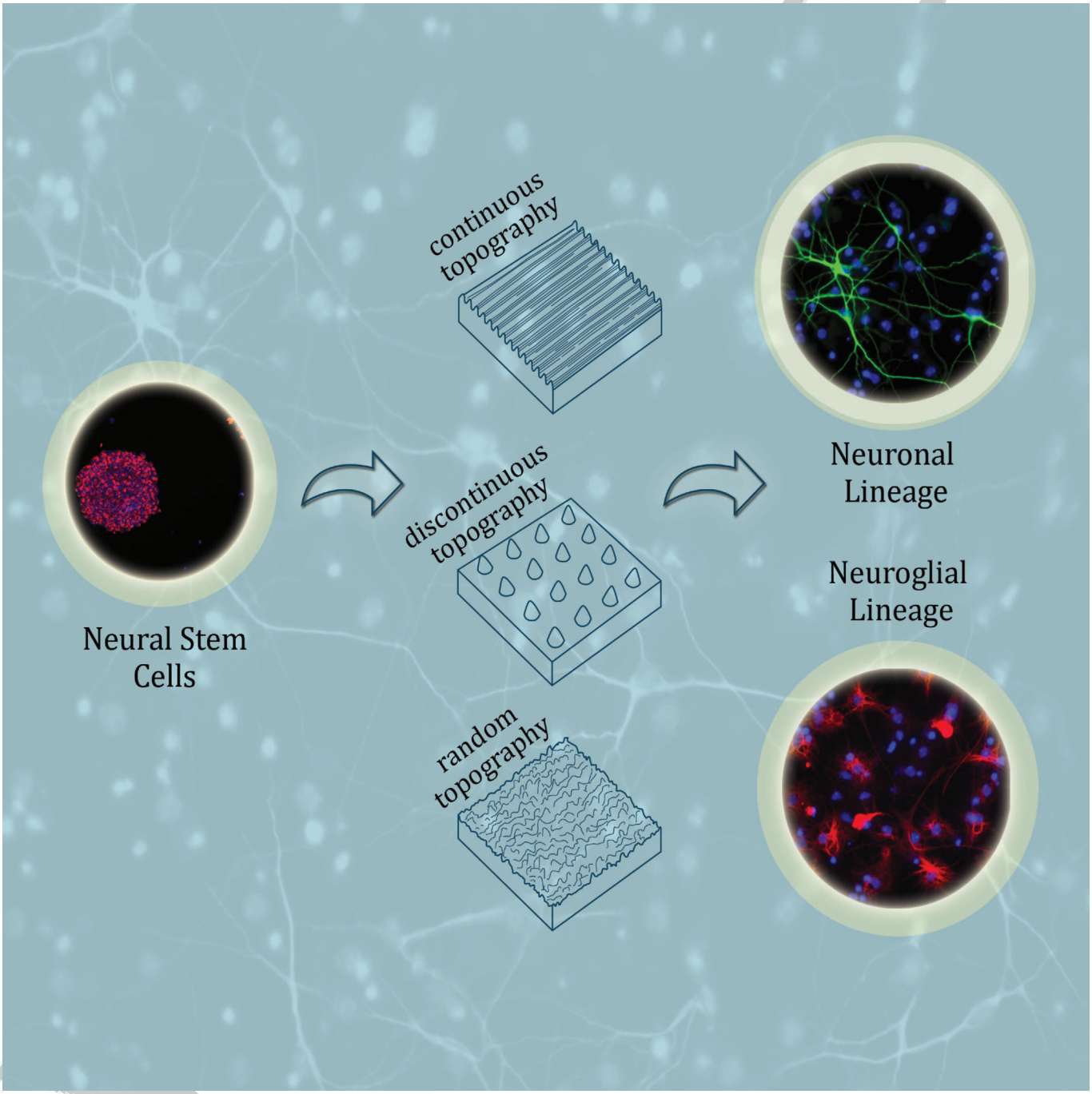

Neural stem cells (NSCs) are self-renewing cells that generate the major cell types of the central nervous system, namely neurons, astrocytes and oligodendrocytes, during embryonic development and in the adult brain. NSCs reside in a complex niche where they are exposed to a plethora of signals, including both soluble and physical signals such as compressive and shear stresses, but also discontinuities and differences in morphology of the extracellular environment, termed as topographical features. Different approaches that incorporate artificial micro- and nano-scale surface topographical features have been developed aiming to recapitulate the in vivo NSC niche discontinuities and features, particularly for in vitro studies. The present review article aims at reviewing the existing body of literature on the use of artificial micro- and nano-topographical features to control NSCs orientation and differentiation into neuronal and/or neuroglial lineage. The different approaches on the study of the underlying mechanism of the topography-guided NSC responses are additionally revised and discussed.

1. Introduction

■■Please give first names and academic titles for all authors ■■Stem cells (SCs) reside in a complex niche where they are exposed to a plethora of signals, including physical signals such as tensile, compressive and shear stresses, discontinuities, and differences in roughness, in extracellular matrix (ECM) composition, etc.[1] The exposure of the SCs on these signals during development and through life seems to impact the outgrowth and their differentiation fate, suggesting that stemness is not solely an intrinsic property of the SCs but also an emergent property arising from their interaction with their environment.[2] Physical stimuli, including topography and mechanical properties, are known to significantly influence stem cell response. Being translated through adhesions, intracellular tension and mechanotransduction, they can alter cell shape or gene expression and thus cell fate.[2,3] Understanding the effect of the SC niche can help towards delineating the signaling mechanisms but also to control the surrounding environment for guiding SC differentiation in tissue engineering applications. Regarding SCs which differentiate into neuronal or glial phenotype, different approaches incorporating artificial micro- and nano-scale surface topographical features, as a way to recapitulate the in vivo SC niche discontinuities and features have been developed and used for in vitro studies. Such studies are presented in the Chapters 2 and 3.

1.1. Neural Stem Cells (NSCs)

Neural stem cells (NSCs) are self-renewing cells that generate the major cell types of the central nervous system (CNS), namely, neurons, astrocytes, and oligodendrocytes, during embryonic development and in the adult brain. The NSCs divide into other NSCs that have conserved their self-renewal capacity and/or into transit-amplifying cells known as neural progenitors that have reduced proliferative potential and a progressively decreasing differentiation potential.[4] Neurogenesis is the process where functional neurons, astrocytes and oligodendrocytes are generated and integrated in the CNS. It was mistakenly believed that, in mammals, it could only occur during embryonic development or shortly after birth and no new neurons could be generated during adulthood.[5] However, in the early 1990s newly generated neurons were identified in the brain of rats by examining the integration levels of 5-bromo-2-deoxyuridine (BrdU) in their brain cells.[6] Meanwhile, Reynolds et al. demonstrated that NSCs isolated from adult rodent brain have self-renewing capacity and may generate neurons and glial cells in vitro.[7]

Early in embryonic development, NSCs do not have any particular organization; instead, they form a single layer of neuroepithelial cells that divide symmetrically forming the neural plate. With the formation of the neural tube, the cells of the neural crest migrate to give rise to a diverse cell lineage including the neurons and glial cells of the peripheral nervous system (PNS).[8] The neuroepithelial cells at a later stage of nervous system development begin to divide assymetricaly with a single neuroepithelial cell giving rise to a typical self-renewing SC and a radial glial cell (RGC) which is characterized by large extending processes and the expression of neuroepithelial and glial markers. With the progression of brain development, the increased population of RGCs forms layers that surround the interior of the neural tube, resulting in the formation of the ventricular zone (VZ). The RGCs continue to divide asymmetrically generating new RGCs as well as intermediate progenitors (also known as "transit-amplifying progenitor cells") that may differentiate into postmitotic neurons and glia. It needs to be highlighted that the aforementioned cell populations interact with other cells of non-neuronal origin (e.g. the surrounding blood vessels, microglia or pericytes)[9] which together with the spatiotemporal expression profile of soluble and insoluble factors and biophysical cues[10] result in a fine-tuned functional nervous system after birth.

Postnatally and during adulthood, some NSC populations permanently reside in specific neurogenic niches. The two most well-described neurogenic niches have been identified in the subgranular zone (SGZ) of the hippocampus[11] and the subventricular zone (SVZ) of the lateral ventricles.[12] Other zones that there is evidence that adult neurogenesis occur include the olfactory bulb, the subcallosal zone underlying the

[a] C. Simitzi, K. Karali, A. Ranella, E. Stratakis
Institute of Electronic Structure and Laser (IESL)
Foundation for Research and Technology-Hellas (FORTH)
Heraklion, 71003 (Greece)
E-mail: simitzi@iesl.forth.gr
stratak@iesl.forth.gr

The ORCID identification number(s) for the author(s) of this article can be found under:
https://doi.org/10.1002/cphc.201701175.

corpus callosum and the cerebellum.[13–15] The NSCs residing in the SGZ and the SVZ generate different types of neurons. NSCs from the SGZ give mostly granule neurons that integrate into the DG of the hippocampus whilst the NSCs of the SVZ produce interneurons that migrate towards the olfactory bulb.

In the SVZ, the quiescent radial glia-like cells (type-B cells) get activated, resulting in the proliferation of the transit-amplifying progenitor cells (type C cells), which increases the number of neuroblasts (type A cells) or glial cells. Type A cells migrate via the rostral migratory stream (RMS) to the olfactory bulb with the assistance of a tube formed by astrocytes. Once they are in the olfactory bulb, the immature neurons abandon radially the RMS, differentiate into different subtypes of interneurons and integrate into local neural networks.[16] In the SGZ, the radial (type I cell) and nonradial (type II cell) precursors proliferate; thus, generating intermediate progenitors which give rise to neuroblasts. From that location, the immature neurons have only to move into the inner granule cell layer and differentiate into dentate granule cells by extending dendrites toward the molecular layer, projecting axons to the CA3 of the hippocampus and integrating into the existing circuitry.[16]

1.2. In Vivo NSCs Niche and Complexity of Its Architecture

The architecture of the neural stem cell niche in vivo is highly complicated, but it is widely accepted that it comprises a specialized microenvironment with specific cellular, biochemical, and physical properties.[17] Its importance resides in the fact that it may determine the fate of a NSC not only by controlling whether it remains in a quiescent state but also by directing its survival, proliferation, migration or differentiation. This specialized microenvironment includes soluble molecules, such as growth factors and hormones, as well as the ECM which is an innate supportive scaffold for the niche (reviewed in [18, 19]).

The NSC niche in vivo contains multiple cell-to-cell interactions within the neighboring cells. For example, in the SVZ there are five distinct cell types that contribute in the mainte-

Dr. Chara Simitzi graduated as a chemical engineer from the National Technical University of Athens and then continued her studies in biomedical and tissue engineering (M.Sc. in Biomedical Engineering- RWTH, Aachen; Ph.D. in Biology- University of Crete). After her Ph.D. she worked at the FORTH Institute in Crete and the QMUL in London. At the moment she is postdoctoral research associate in the Applied Biomedical Engineering group at the UCL in London. Her scientific interests focus on the cell-biomaterial interface and more specifically on the development of novel types of scaffolds for tissue engineering applications and cell culture platforms for in vitro studies to address cell biology questions.

Dr Anthi Ranella is Assistant Researcher at the Foundation for Research and Technology-Hellas (FORTH). She graduated the Department of Biology at the University of Crete. She received the Master degree in Molecular Biology and the Doctorate degree in Biomedicine from the Biology Department of University of Crete. She is currently leading the Tissue Engineering and Regenerative Medicine research group at IESL-FORTH. Her current research interests are the Biomedical Applications of Laser in Tissue Engineering-Regenerative Medicine, Diagnostics and Drug Delivery. Her research activities have led to the granting of 2 patents and have contributed to over 30 publications in international peer-reviewed journals, 4 chapters in scientific books and have been cited over 1250 times (h-factor = 16:Google Scholar).

Dr. Kanelina Karali received her B.Sc. in Biology from University of Athens and then continued her studies at University of Edinburgh (UK) where she obtained her M.Sc. and Ph.D. in Neuroscience. Her research interests focus on the concepts of neuroregeneration and neuroprotection in neurodegenerative diseases (i.e. Alzheimer's disease) or trauma (i.e. spinal cord injury). She is interested in the study, manipulation and exploitation of stem cells and unveiling their neuroregenerative potential either pharmacologically or in the context of neural tissue engineering.

Dr. Emmanuel Stratakis is Research Director at the Foundation for Research and Technology-Hellas (FORTH). He received his Ph.D. in Physics from the University of Crete in 2001 and then he joined the University of California Berkeley as a visiting researcher. He is currently leading the Ultrafast Laser Micro- and Nano- Processing group of FORTH (http://www.iesl.forth.gr/ULMNP). He has over 130 SCI publications, 4500 citations and he has coordinated many National and EU grants. Since 2015, he directs the European Nanoscience Facility of FORTH, part of the NFFA-Europe EU Infrastructure, where he is a member of the General Assembly. He is a member of the COST Scientific Committee and National Expert in the NMBP Program Committee of the Horizon 2020.

nance of the specialized niche microenvironment and confer its unique regenerative potential namely the type A, B and C cells, the ependymal cells and a vascular endothelium.[20] A single layer of ependymal cells line the ventricle forming a barrier between the brain parenchyma and the cerebrospinal fluid.[21] The NSCs lie just under the ependymal cell layer and maybe in contact with the cerebrovascular fluid with a single apical process. Furthermore, there is evidence that the vasculature is linked with neuronal development not only by synchronization of angiogenesis and neurogenesis but also by the secretion from the RGCs of growth factors that are involved in the development of the vasculature, such as the vascular endothelial growth factor (VEGF)[22] and the production by the endothelial cells of neurogenic factors such as VEGF, neurotrophin-3 (NT3) and Jagged-1 (a Notch ligand) (reviewed in Ref. [23]). One study has also shown that in the transcriptome of mouse brain endothelial cells several genes potentially relevant to the NSCs have been flagged.[24] Finally, a very recent study showed that mimicking the vasculature scaffold facilitates NSCs migration in vitro.[25]

The ECM, together with the basal lamina, is a key component of the neural stem cell niches. The ECM provides physical, chemical, and mechanical support for the cells and contains supermolecular assemblies of proteins and glycosaminoglycans, which play a vital role in the cell behavior.[19] They act as a supportive scaffold seeded with the various cell types, growth factors and ECM molecules. Some of these ECM molecules such as laminin, collagen IV, perlecan, the glycoprotein tenascin C, the chondroitin sulfate proteoglycans (CSPG), and the heparan sulfate proteoglycans (HSPG) have crucial roles for the maintenance and the function off the NSCs.[26] Laminin is an ECM heterotrimeric protein highly abundant at the basal lamina. Through its receptor $\alpha6\beta1$ integrin laminin mediates the adhesion of NSCs to the ECM. Moreover, it can be located at the "fractones" of the SVZ which are branches, or "finger-like processes that extend from the ependymal cells and blood vessels of the mammalian brain.[9] In addition, fibroblast growth factor-2 (FGF-2), which is a growth factor crucial for NSCs survival, binds to HSPG, CSPG, and perlecan indicating that these components of the ECM affect growth factor activity and subsequently the maintenance of the NSC niche.[27] Tenascin C, an extracellular matrix glycoprotein, is also an important ECM component produced by type B cells, the astrocytes involved in the migration of type A cells and the RGCs. It controls the responsiveness of NSCs to epidermal growth factor (EGF) and FGF-2.[28]

Finally, there is growing evidence that physical parameters, such as tissue topography defined by the organization of the ECM, the vasculature, and cellular processes,[25] shear forces and elasticity/stiffness, also have a significant effect on NSC niche maintenance and function.[18]

1.3. Cell Types, Assays, and Materials

Cell Types

As mentioned above, NSCs are multipotent stem cells having the capacity to proliferate, self-renew, and terminally differentiate into the three major cell types of the CNS, that is, neurons, oligodendrocytes, and astrocytes (multipotentiality). NSCs can be isolated from both the embryonic and the adult CNS. Another source of NSCs is embryonic stem cells (ESCs), that is, the truly pluripotent SCs which can generate any tissue of the body.[29] Embryonic NSCs have been isolated from the embryonic mammalian CNS (i.e. hippocampus, cerebral cortex, basal forebrain) as well as from the PNS (i.e. neural crest). Adult NSCs can be isolated by the two principal adult neurogenic regions, the hippocampus and the SVZ, and some non-neurogenic regions, including spinal cord.[30]

To convert the aforementioned tissue sources into NSCs, cells derived from fetal, adult, or ES sources are cultured in media containing mitogens, such as EGF and FGF-2. NSCs from these sources can be expanded as either adherent monolayers or spherical aggregates, termed "neurospheres". The neurospheres (NS) are spheroid structures that consist of cells with a rich ECM. NS are enriched for $\beta1$ integrins, epidermal growth factor receptor (EGFR), and cadherins.[31,32] NS produce their own ECM molecules (laminins, fibronectin, chondroitin sulphate proteoglycans) and growth factors.[33] Initial cell-to-cell contacts are retained by dividing cells in suspension cultures. Moreover, they can be subsequently dissociated to produce a new neurosphere.[34]

To promote NSC differentiation, the mitogens are usually replaced by specific morphogens or growth factors, such as NT3, neurotrophin-4 (NT4), bone morphogenetic protein (BMP), and ciliary neurotrophic factor (CNTF). These factors promote initial maturation into either neurons or glia.[35,36] Final differentiation into specific neuron and glial types can be induced by other morphogens and growth factors, and in some cases transcription factors. For example, 1) brain-derived neurotrophic factor (BDNF) and sonic hedgehog (Shh) for gamma-aminobutyric acid (GABA) neurons, 2) FGF-8, Shh for domapine neurons, 3) retinoic acid (RA) and Shh for motor neurons, 4) CNTF, leukemia inhibitory factor (LIF) and BMPs for astrocytes and 5) purmorphamine (PMN), vitronectin (VN), platelet-derived growth factor (PDGF), cyclic adenosine monophosphate (cAMP), FGF-2 for oligodendrocytes are used.[35,36] In the studies presented in this paper, NSCs were either treated with the well-established differentiation media or with no special growth medium (spontaneous or direct differentiation processes). In these two different approaches the role of topographical cues 1) in synergy with the biochemical signals, or 2) as a sole agent on NSC differentiation fate was investigated.

Apart from the above NSC sources, human mesenchymal stem cells (hMSCs) have been reported to *trans*-differentiate into neuronal-like cells upon culture in neuronal induction media,[37,38] although the mechanism is not well understood.[2]

Assays

To investigate the effect of topography on NS cellular functions, different cell assays have been used, ranging from cell adhesion and neurite outgrowth assays to more complex functional assays, such as cell differentiation on the different topographies. Cell viability was assessed via metabolic cell viability assays or via measuring the calcein-AM- and Ethidium Homodimer-1 (EthD-1) positive cells, while cell proliferation was assessed via measuring the cell number or via well-established metabolic cell proliferation assays, like MTT (3-(4,5-Dimethylthiazol-2-yl)-2,5-Diphenyltetrazolium Bromide) or via cellular markers for proliferation (e.g. BrdU integration and Ki67). In order to assess stem cell adhesion on the different topographies, the expression of specific adhesion protein markers, such as the focal adhesion actin-associated proteins, like focal adhesion kinase (FAK)[39] or vinculin[40] was investigated.

The differentiation of NSCs into specific fate can be evaluated by the expression of protein markers specifically expressed on the terminally differentiated cells. Such specific protein markers are neuron-specific class III beta-tubulin (Tuj1) for neurites on early neurons, neurofilament (NF) expressed on neurites and microtubule-associated protein 2 (MAP2) expressed on neuronal cell bodies of postmitotic neurons, glial fibrillary acidic protein (GFAP) for astrocytes and oligodendrocyte transcription factor 1 (Olig1), O4, 2′,3′-Cyclic-nucleotide 3′-phosphodiesterase (CNPase), RIP, and myelin basic protein (MBP) for oligodendrocytes. Nestin is used as the main marker to identify neural precursors. Upon stem cell differentiation, nestin expression is downregulated and replaced by other intermediate filament proteins, such as neurofilaments in neurons and GFAP in astrocytes.[41] In the case of ESCs, the positive expression of the differentiation markers shall be accompanied by the simultaneous negative expression of the respective markers for pluripotency, like octamer-binding transcription factor 4 (Oct4) and stage-specific embryonic antigen 1 (SSEA-1). An additional marker for assessing the neuronal differentiation is measuring the levels of released nitric oxide.[37,42] Except for the protein, gene expression analysis (e.g. via Polymerase chain reaction-PCR) can provide valuable information on the differentiation state of the NSCs. In order to assess the functionality of the differentiated cells, expression of synaptic markers (e.g. synaptophysin, etc.), synaptic transmission, and electrophysiological properties of these were evaluated. Furthermore, morphological analysis of the differentiated cells on the patterned substrates was assessed via SEM.

Materials

Different materials patterned on different topographies have been developed and used for studying the effect of topography and regulating NSC functions. Electrospun polymeric fibers made of mostly poly-L-lactide (PLLA)[43] and polycaprolactone (PCL)[39,44,45] have been used. Other polymers are polyethersulfonate[46] and carbon nanotubes (CNT).[43] Alternating grooves and ridges were made in silicon[47] via photolithography and then copied from the initial masters to softer polymeric materials, such as polydimethylsiloxane (PDMS)[38,48,49] via soft lithography techniques.[47]

2. The Effect of Topographical Cues on Neural Stem Cells

The stem-cell responses, including adhesion, morphology, proliferation, and differentiation to different continuous, discontinuous, and random roughness topographies are summarized in Tables 1, 2 and 3, respectively. The classification of the topographies into continuous, discontinuous and random was introduced in our previous review paper.[50] Briefly, primary classification categorizes the various deterministic pattern geometries into continuous and discontinuous. A second classification divides further the continuous geometries into anisotropic and isotropic topographies. The first are directionally dependent, providing cues preferentially along a single axis, such as in the case of parallel aligned fibers or grooved substrates. In the case of the random surface patterns, the surface topography is usually described in terms of statistical roughness parameters, such as the root mean square (Rq) value. Tables 1–3 include information about the topographical pattern, biomaterial and the respective stem cell responses of the various studies which are organized with increasing topographical feature size. Studies of NSCs and ESCs towards neuronal and/or neuroglial fate are mainly presented. Two studies with mesenchymal stem cells (MSCs) towards neuronal lineage are also included.

2.1. The Effect of Continuous Topographies on Neural Stem Cells

Effect of Continuous Topographical Cues on Cellular Shape and Orientation/Alignment

Continuous topographies, such as alternating grooves and ridges, gratings, and parallel fibers have been shown to influence cellular shape and orientation, as these changes can be manifested by cytoskeletal rearrangement and nucleus elongation. NSCs on silicon linear or cyclic anisotropic micropatterns of 2 or 10 μm width and 4 μm depth aligned and elongated along the direction of the grating axis (Figure 1 A).[51] Focusing on neurite outgrowth and alignment, the continuous anisotropic topographies have an important guidance effect. Lee et al. reported the alignment of the extended neurites from the differentiated hESCs along the direction of 350 nm nanogrooved patterned substrate.[52] Bedeuer et al. cultured hNSCs on PDMS deep (25 μm) grooves of increasing groove width, ranging from 5 to 60 μm.[49] They showed that there is a critical width value, associated with the mean soma diameter (12 ± 3 μm), which introduces two regimes of cellular responses (Figure 1 B). Cells on micropattern widths larger than soma diameter exhibited one, two or at least three neurites, which were quasi-equally distributed, showing a similar response to that obtained on a non-patterned surface. Notably, for micropattern width smaller than this value, stem cells extended fewer neurites which were strongly aligned along the microchannels.[49] The study reports the preferential alignment of the neurites

Table 1. a) The effects of artificial micro- and nanotopographies on NSCs' continuous topographies (grooves or gratings).

Feature Type	Biomaterial/Fabrication Technique	Feature dimensions	Cell type/Cell assay	Substrate Treatment/ Protein Coating	Cellular response	Ref.
Grooves	Polyurethane Acrylate/ UV-assisted capillary force lithography	Width: 350 nm Spacing: 350 nm Depth: 500 nm	hESC/ Direct differentiation (without the use of differentiation agent)	Oxygen plasma treatment/ Gelatin	Effect on differentiation: hESCs differentiated preferentially into neuronal but not into glial lineage after 5DIV in the absence of differentiation-inducing agents. ESCs were negative for brachyury (mesoderm marker) and Pdx1 (endoderm marker).	[52]
Gratings	PDMS/ Soft lithography	Nanogratings Width:0.25–2 μm Pitch: 0.25–2 μm Depth:0.25–2 μm Microgratings Width:1-2 μm Pitch: 1-2 μm Depth:0.08–2 μm	hESCs/ Direct differentiation (without the use of differentiation agent)	Poly-ornithine & Laminin	Effect on orientation: Cells elongated and aligned along the grating axis. Effect on differentiation: Neuronal differentiation of hESCs was promoted after 7DIV without the use of specific differentiation agents. Among the different anisotropic patterns, cells on the nanogratings showed the highest MAP2 expression. Compared with the conventional differentiation (via RA), neurons after direct differentiation exhibited longer neurites.	[48]
Grooves	PLGA/ Solvent-assisted Capillary Force Lithography	P400: Width: 400 nm Spacing: 400 nm Depth: 600 nm P800: Width: 800 nm Spacing: 800 nm Depth: 600 nm P5000: Width: 5000 nm Spacing: 5000 nm Depth: 5000 nm	hNSCs/ Spontaneous differentiation or inclusion of NGF	PLL and Fn or DOPA, PLL and Fn (via sequential immersion)	Effect of topography on focal adhesion: Increased vinculin expression on grooved substrates compared to the flat at 4d; the effect was more intense with decreasing groove size. Effect of topography on cell alignment: Enhanced cytoskeletal alignment along the grating axis of the patterns on all grooved substrates; cells were randomly oriented on the flat substrates. Effect of surface coating on focal adhesion and alignment: DOPA coating enhanced focal adhesion and F-actin alignment. Effect of topography and surface coating on differentiation: Neuronal differentiation was enhanced on the nanogrooves (P400, P800) compared to the flat and the micropatterns (P5000) in both spontaneous and neurotrophic conditions at 4d. DOPA coating potentiated this effect. Combination of nanotopography and neurotrophic signals was the best.	[55]
Nanopored microgrooves	PS-b-PMMA/ Photo-lithography (micropattern) Reactive ion etching (nanopattern)	Micropattern: Width:1.5 μm Pitch: 1.5 μm Depth:0.625 μm Nanopattern: Pore size:10 nm Pore spacing: 28 nm	Human telencephalon NSCs/ Spontaneous differentiation conditions	Fibronectin	Effect on cytoskeleton alignment: In contrast to the flat substrate (FS) or nanopatterned substrate (NPS), NSCs on both the micro (MPS)- and hierarchical (HPS) patterned substrates exhibited a highly elongated cytoskeleton along the patterned groove. Effect on focal adhesion: Focal adhesion formation of hNSCs was significantly enhanced on the HPS compared to other substrates. Effect on differentiation: Compared to the other substrates, the population of neuronal lineage cells was increased on the HPS, whereas the relative population of astrocytes was concurrently decreased on the HPS.	[40]
Linear (LMP-Grooves) & circular (CMP) patterns	Silicon/ Photo-lithography	Width: 10/2 μm Spacing: 10/2 μm Depth: 4 μm	ANSCs/Differentiation induced by GM supplemented with FBS and RA	Poly-ornithine and Laminin	Effect on alignment: Cell nucleus elongated along the axis of the features; cells extended branches guided by topological directionality on LMP and CMP. Effect on proliferation: Proliferation rates on both LMP and CMP were significantly decreased compared to control Effect on differentiation: On both the LMP and CMP the differentiation towards neurons and oligodendrocytes was increased compared to the flat. On the contrary, the differentiation towards astrocytes was decreased. This effect was more pronounced on the smaller feature size (2 μm vs. 10 μm).	[51]

Table 1. (Continued)

Feature Type	Biomaterial/Fabrication Technique	Feature dimensions	Cell type/Cell assay	Substrate Treatment/ Protein Coating	Cellular response	Ref.
Grooves	PDMS/ Soft lithography	Width: 5/10/20/60 μm Spacing: 5/10/20/10 μm, respectively Depth: 25 μm	Adult hNSCs/ Differentiation induced by GM supplemented with B27 nutriments and NGF	Oxygen plasma treatment/ Poly-lysine and laminin	Effect on growth and positioning: Cells were found inside the grooves Effect on neurite alignment: The smaller the channel width, the better the neurite alignment and the smaller the number of neurites per cell. Effect on differentiation: Cells differentiated on both neurons and astrocytes on the micropatterned surface. For feature widths smaller than the soma diameter, neuronal differentiation was affected (i.e. less neurites, less branching). For feature widths larger than soma diameter, the differentiation rates obtained were comparable to that on a non-patterned surface.	[49]
Gratings	PDMS/ Soft lithography	Nanopattern: Width: 0.35 μm Pitch: 0.7 μm Depth: 350 nm Micropatterns: Width: 1/10 μm Pitch: 2/20 μm, Depth: 350 nm	hMSCs/ Differentiation was induced by GM supplemented with RA	Collagen	Effect on proliferation: Proliferation decreased with decreasing width size Effect on differentiation: MSCs on nanopatterned samples exhibited significant up-regulation of neuronal markers, compared to micropatterned and unpatterned substrates. MSCs on the nanopatterned samples expressed mature neuronal markers even without the chemical induction medium.	[38]
Grooves	Hydrogenated amorphous carbon (a-C:H)/ Radiofrequency plasma-enhanced chemical vapor deposition (rf-PECVD)	200P Width:40 μm Spacing: 80 μm Depth: 24 nm 300P Width:30 μm Spacing: 40 μm Depth: 24 nm 400P Width:20 μm Pitch: 30 μm Depth: 24 nm	hBone marrow Stem Cells/ Differentiation was induced by GM supplemented with BDNF, β-FGF and PDGF-AA		Effect on protein adsorption: Uniform a-C:H > nanopattern a-C:H (200P≅400P≅300P) > glass coverslip and TCP. Effect on cell morphology: Cells assumed an elongated morphology only on the ridge-patterned films, whereas cells maintained a fibroblast-like morphology on smooth surfaces (uniform response on a-C:H, TCP and glass). Effect on differentiation: In the absence of chemical stimulus (ie. BDNF) only the 300P substrate promoted hBMSCs differentiation. In the presence of BDNF, neuronal differentiation into neuronal lineage was increased on the 300P compared to 200P and 400P.	[37]
b) The effects of artificial micro- and nanotopographies on NSCs- Continuous Topographies (Fibers)						
Feature Type	Biomaterial/Fabrication Technique	Feature dimensions	Cell type/Cell assay	Treatment/ Protein Coating	Cellular response	Ref.
Fibrils	Collagen/CNT composite/ Mixing/Blending & Gelation	Diameter: 35-55 nm (compared to 5-15 nm of the pure collagen)	hESCs/ Spontaneous differentiation conditions		Effect of orientation: Cells on collagen/CNT mostly grew long bipolar filaments along the side of the well-oriented thick fibril bundles, whereas cells on pure collagen grew filaments frequently branching and extending along variable directions. Effect on spontaneous differentiation: Cells on the collagen/CNT matrix demonstrated significantly higher level of nestin than those on the pure collagen matrix, regardless of the similarity in cell shape in the two cases.	[58]
Random & aligned fibers	PCL/ Electrospinning	Diameter: 250 nm	1) mESC and 2) Embryoid Bodies (EBs)/ Differentiation induced by GM supplemented with RA	No	Effect on migration out of the EBs: Cells migrated away from the EB along the long axes of the aligned PCL nanofibers. In contrast, cells cultured on random PCL nanofibers remained more localized to the region of the EB's main body. Effect of alignment: Neurite extension and oligodendrocyte migration was guided by the direction of nanofiber alignment. Effect on differentiation: i) Embryoid bodies: The number of cells expressing neuronal and oligodendrocyte markers was higher on the aligned compared to the random fiber substrates. On the contrary, the number of cells expressing astroglial marker was smaller on the aligned compared to the random fiber substrates (14DIV); ii) ESCs without forming EBs: Neuronal differentiation was successful.	[44]

Table 1. (Continued)

Feature Type	Biomaterial/Fabrication Technique	Feature dimensions	Cell type/Cell assay	Substrate Treatment/ Protein Coating	Cellular response	Ref.
Random fibers-Hybrid scaffold	PCL fibers coated with Graphene Oxide (GO)/ Electrospinning	Diameter: 200-300 nm	aNSCs	Laminin	Effect on differentiation: Selective differentiation of NSCs into oligodendrocytes in a GO concentration-dependent way. The results support a role of GO-coating in the upregulation of these downstream molecules in the integrin signaling pathway.	[39]
Random & Aligned Fibers	PLLA/ Electrospinning	Diameter: micro:1250 nm nano: 250 nm	Neonatal mNSCs/ Differentiation induced by GM containing N2 supplement		Effect on cell morphology and neurite outgrowth: NSCs on the aligned fibers elongated along with the fiber direction independent of the fiber diameter. NSCs on the randomly oriented fibers extended multiple processes. Effect on differentiation: Increased differentiation on nanofibers compared to that on the microfibers, independent of the fiber orientation.	[53]
Random Fibers	Poly-ethersulfone/ Electorspinning	Diameter: "283-nm": 283 ± 45 nm "749-nm": 749 ± 153 nm "1452-nm":1452 ± 312 nm	Adult rNSCs/ Differentiation with the supplementation of RA and FBS	Laminin	Effect on viability: NSCs cultured on fibers with a diameter of 1452 nm showed lower viability by day 5. Effect on proliferation: Proliferation decreased with increasing fiber diameter. Effect on morphology: While cells on "283-nm" were able to spread along the nanofiber matrix randomly and assumed cell morphology of glial lineage, cells on larger fibers extended on single fibers due to the size restriction. Effect on differentiation: On "283 nm"fibers, there was a 3-fold increase in the percentage of oligodendrocytes compared to the control. In contrast, NSCs on the "749 nm" yielded the highest fraction of neuronal differentiation among all substrates.	[46]
Parallel or random fibers	PCL/ Electrospinning	Diameter (nm): 260; 480; 930	Adult rNSCs/ Differentiation with RA or IGF/Noggin	PLO and laminin	Effect of fiber orientation: ANSCs on aligned fibers elongated along the major fiber axis. Upon induction of differentiation with RA, more cells on aligned fibers exhibited markers of neuronal differentiation as compared with cells on random fiber or unpatterned surfaces. Effect of topography on survival: Aligned fiber substrates were less receptive to the attachment and continued survival of oligodendrocytes than random fiber or unpatterned substrates.	[56]
Random Fibers	PCL/ Electrospinning	Diameter: 750 ± 100 nm	Adult rNSCs/ Differentiation with FBS	Treatment with Ethylene-diamine	Effect on differentiation: NSCs differentiated preferentially into oligodendrocytes.	[45]
Parallel aligned fibers	PLLA with SWCNT or MWCNT/ Electrospinning	Diameter: PLLA/SWCNT: 450 nm PLLA/MWCNT: 500 nm PLLA: 500 nm	mESCs/ Culture in neural induction medium	Oxygen plasma treatment	Effect on viability: Cell viability was the same on all fibers. Effect on orientation: Differentiated mESC aligned along the underlying fibers. Effect on differentiation: Significant upregulation of neuronal markers on the composite-fibers compared to pure PLLA fibers. Nestin expression was the same with the one on PLLA fibers.	[43]
Parallel aligned fibers	PCL/ Electrospinning	Small Diameter (μm): 0.86 ± 0.45 Large Diameter (μm): 8.8 ± 6.5	E13 mNSC Neurosphere formation	PDL or PDL and Laminin	Effect of fiber diameter on cell morphology: Smaller-fiber topography, supported cell migration (10 DIV), independent of coating; individual cells showed alignment to the fiber mats. Large-fiber topography without laminin prevented cell migration. Effect of laminin coating on migration: Large-fiber topography without laminin prevented cell migration. Laminin coating of both the large and smaller-fiber patterns supported cell migration. Effect of topography on cell differentiation/morphology: Cells on the small fibers exhibited fibrous/bipolar morphology or multipolar morphologies; cells on the large fibers showed predominantly fibrous/bipolar morphology.	[25]

Table 1. (Continued)

Feature Type	Biomaterial/Fabrication Technique	Feature dimensions	Cell type/Cell assay	Substrate Treatment/ Protein Coating	Cellular response	Ref.
Random fibers	SWNT-PLGA composite/ Electrospinning (PLGA) Vacuum impregnation post-processing (SWNT)	PLGA Diameter: 1.2 μm SWNT-PLGA Diameter: 2.9 μm	iPSCs/ Differentiation induced by GM containing *N*-2 supplement	Oxygen plasma, PDL and laminin	Effect on differentiation: SWNT-PLGA composite enhanced neuronal differentiation of NSCs compared to PLGA controls without SWNT	[57]

Abbreviations: a: Adult; BDNF: Brain-derived neurotrophic factor; CNT: Carbon Nanotube; DIV: Days in vitro; DOPA: 3,4-dihydroxy-L-phenylalanine; EB: Embyoid Body; ESC: Embryonic stem cells; FGF: Fibroblast Growth Factor; FBS: Fetal Bovine Serum; Fn: Fibronectin; GM: Growth Medium; h:Human; iPSCs: Induced pluripotent stem cells; NGF: Nerve Growth Factor; NSCs: Neural Stem Cells; PCL: Polycaprolactone; PDMS: Polydimethylsiloxane; PDGF: Platelet-derived growth factor; PDL: Poly-D-lysine; PLGA: poly(lactic-co-glycolic acid); PLL: Poly-L-lysine; PLLA: Poly-L-lactide; PMMA: Poly(methyl methacrylate); PS: Polystyrene; r:Rat; RA: Retinoic Acid; Si: Silicon; UV: UltraViolet. **Comment**: For reasons of clarity and ease of comparison, the grooved-/ridged- patterns are presented with respect to the groove (even if the authors have reported them with respect to the ridges).

Table 2. The effects of artificial micro- and nanotopographies on NSCs' discontinuous topographies.

Feature Type	Biomaterial/ Fabrication Technique	Feature dimensions	Cell type/Cell assay	Treatment/ Protein Coating	Cellular response	Ref.
Pillars & wells	PDMS/ Soft lithography	Pillars: Width: 1 μm Pitch: 6.5 μm Height: 1 μm Wells: Width: 2 μm Pitch: 12 μm Depth: 2 μm	hESCs/ Direct differentiation (without the use of differentiation agent)	Polyornithine & Laminin	Effect on differentiation: Both isotropic patterns promoted the glial rather than the neuronal differentiation of hESCs compared with the control and the anisotropic continuous patterns (see Table 1); however into different glial subtypes/ subpopulations: More hESCs differentiated into oligodendrocytes and astrocytes on pillars and wells, respectively.	[48]
Dot Micropatterns (DMP)	Si/ Photo-lithography	Quadrant-dot shape Width:10/ 2 μm Pitch: 10/ 2 μm, respectively Depth:4 μm	Adult rNSCs/ Differentiation: GM supplemented with RA and FBS	Poly-L-ornithine & Laminin	Effect on orientation: There was no obvious preference of the direction of alignment and extension for those cells cultured on the DMP with both 2 and 10 μm width and control substrates. Effect on proliferation: NSCs on DMP exhibited decreased proliferation compared to the control substrates. Effect on differentiation: NSCs on DMP exhibited similar differentiation response compared to the control unpatterned substrates. Increased differentiation towards astrocytes, while decreased differentiation towards neurons and oligodendrocytes compared to the flat and the anisotropic continuous patterns (See Table 1).	[51]
Honeycomb pattern	PCL & amphiphilic polymer (Cap) blend/ Casting and controlled evaporation	Pore size: 3–15 μm	E14 mNSCs/ GM with 2-mercaptoethanol	Poly-L-lysine	Effect on differentiation: Membranes with a pore size of 3 and 5 μm suppressed the differentiation of the NSCs. The number of differentiated cells increased with increasing pore size.	[59]

Abbreviations: a: Adult; DIV: Days in vitro; ESC: Embryonic stem cells; FBS: Fetal Bovine Serum; GM: Growth Medium; h: Human; NSCs: Neural Stem Cells; PCL: Polycaprolactone; PDMS: Polydimethylsiloxane; RA: Retinoic Acid; Si: Silicon

along the edge at the bottom of the microchannel, more striking for the smaller widths, suggesting that the channel width is a critical parameter for neurite outgrowth and stem cell development.[49] Yang et al. used a hierarchical topography (HPS) consisting of a PS-b-PMMA nanopore-patterned micro-grooved topography (pore spacing/size: 28/10 nm; groove spacing/ width: 1.5/1.5 μm). NSCs cultured on both the micro-grooved topography (MPS) and the HPS were highly aligned along the

Table 3. The effects of artificial micro- and nanotopographies on NSCs' random topographies.

Feature Type	Biomaterial/ Fabrication Technique	Feature dimensions	Cell type/Cell assay	Treatment/Protein Coating	Cellular response	Ref.
Nano-roughness	Silica (SiO_2) nanoparticles/ Stoeber process	Monodispersed silica colloids of increasing size (R_q: 12 −80 nm)	E15.5 rNSCs/ N2 media or CNTF (promotes differentiation of NSCs to astrocytes)	Poly-lysine	Effect on differentiation: On the Rq of 32 nm and 16 nm there was a 10- to 20-fold greater number of NSCs showed spontaneous differentiation to neurons. Even upon exposure to CTNF, a twofold increase in NSCs positive for the neuron-specific class III β-tubulin, compared to glass.	[62]
Nano-grained roughness	Ultra-nanocrstalline diamond film/ microwave plasma chemical vapor deposition (MPCVD)	Grain size: 5 nm	E11.5 mNSCs/ Low serum medium or differentiation medium	Hydrogen- terminated (by hydrogen treatment)	Effect on differentiation: NSCs on the H-UNCD expressed markers of neurogenic, astrocyte and oligodendrocyte lineage in both basal and differentiation medium. NSCs on PS (control) expressed only markers of astrocytic lineage in both basal and differentiation medium. Effect on adhesion: NSCs on H-UNCD were spread more extensively than those on PS; filopodia on H-UNCD showed longer extensions and more protruded than on PS. Effect on fibronectin adsorption: Increased fibronectin adsorption compared to that on the flat (PS).	[66]
Nano-roughness	Nanodiamonds monolayer	R_q: 3.74 nm	HNSCs/ Neurobasal medium	Oxygen (by ozone treatment) or hydrogen (by hydrogen anneal process)-terminated with and without PL + LN	Effect on surface chemistry: NSCs on (protein-coated) oxygen-terminated, but not on hydrogen-terminated, nanodiamonds showed a good cell attachment, which was comparable to that on (protein-coated)TCPS with the same nanoroughness.	[64]
Porous nano-pattern	TiO_2/ Sintering; PDMS/ Soft lithography	Porous diameter: 200-500 nm	E13.5 rNSCs/ Neural differentiation (by removing bFGF and EGF from the culture medium)	PDL and laminin	Effect on differentiation: NSCs porous-TiO_2 showed decreased neurogenic differentiation and increased astrocyte differentiation, compared with the flat TiO_2 or TPCS, after 21dayss. Effect on astrocyte morphology: NSCs on porous TiO_2 differentiated into fibrous astrocytes, while NSCs on TCP and Flat differentiated into protoplasmic astrocytes	[63]

Abbreviations: CNTF: ciliary neurotrophic factor; ESC: Embryonic stem cells; GM: Growth Medium; h: Human; m: mouse; LN: Laminin; NSCs: Neural Stem Cells; PDL: Poly-D-lysine; PDMS: Polydimethylsiloxane; PL: polylysinePS: polystyrene; r: rat; Si: Silicon; TCP: Tissue culture plastic; TPCS: Tissue plastic culture substrate.

patterned groove, compared to the flat and the nanopatterned substrate (NPS). These results suggest that the micro-scale compared to the nano-scale of the topographical feature is the critical factor for cell orientation and alignment (Figure 1C).[40]

Neurite outgrowth and alignment were also shown to be influenced by parallel-aligned polymeric fibers of submicron-to-micron diameter.[44,53] Using aligned PLLA microfibers (diameter: 1250 nm) and nanofibers (diameter: 250 nm), Yang et al. showed that cells exhibited mostly bipolar shape and neurites aligned along the fiber axis with less branching between the fibers (Figure 1D).[53] On the contrary, cells exhibited multiple processes and the neurites were randomly oriented on the respective micro- and nanofibers of random orientation.[53] Fibers of larger diameter, such as 10 μm, induced migration of precursors out of the neurosphere along fibers in a chain-like pattern.[25] This organization of the cells into a chain-like arrangement along the fibers has been previously reported in dissociated Schwann cells cultured on 15 μm diameter chitosan fibers.[54]

Effect of Continuous Topographical Cues on Stem Cell Differentiation

An increasing number of studies report the effect of micro- and nano-scale continuous topographies on differentiation of NSCs and ESCs into neuronal or neuroglial cells. Importantly, topographical cues may selectively enhance NSCs differentiation to specific lineage. Christopherson et al. studied the effect of fiber diameter of polyethersulfone electrospun substrates on NSC differentiation and proliferation, showing that different

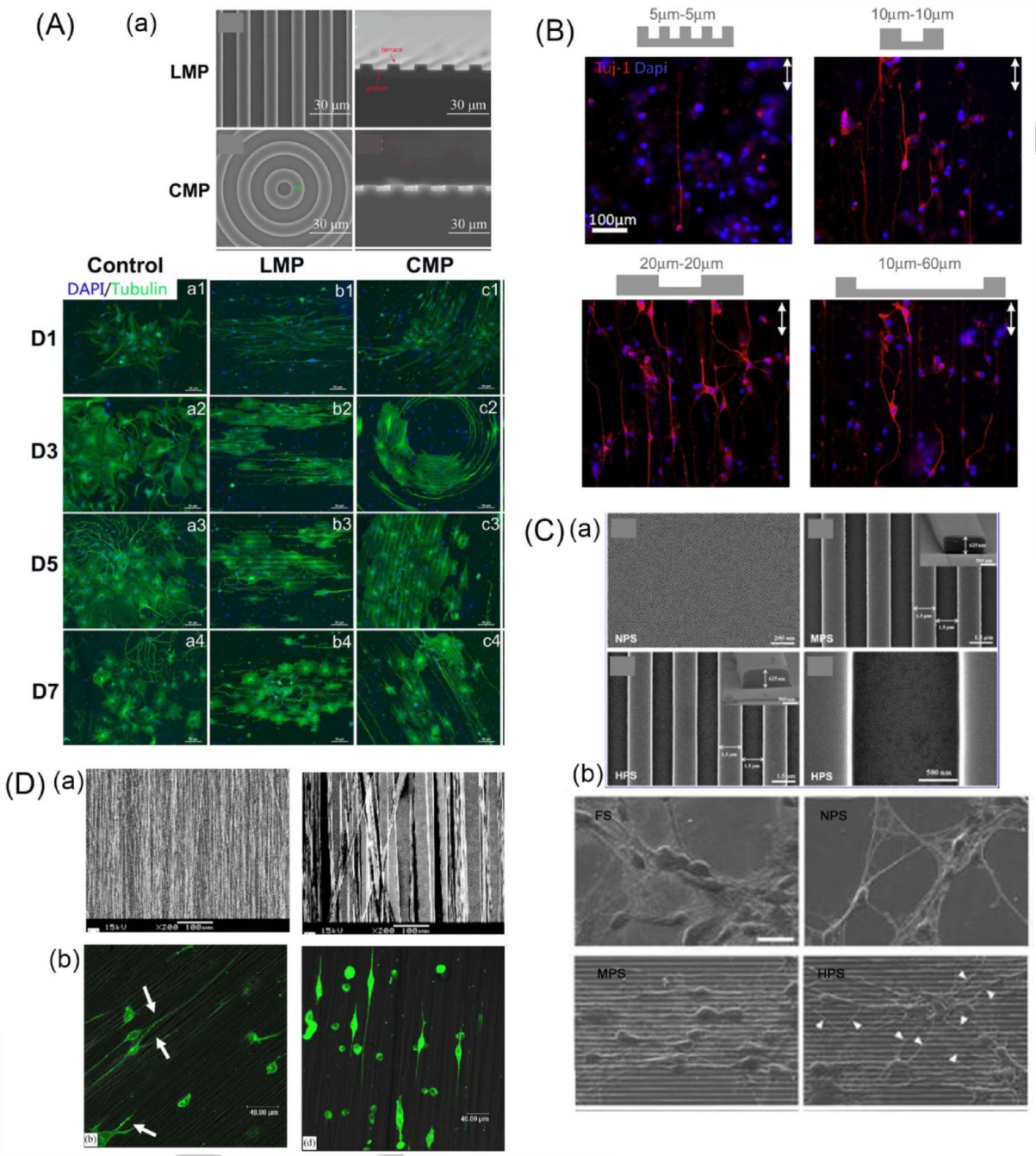

Figure 1. Aa) SEM images of the anisotropic linear (LMP) and cyclic (CMP) silicon micro-patterns; Ab) Fluorescence microscopy images of the NSCs on the control and the LMP and CMP substrates for different days from 1–7 (D1-D7) (Reprinted with permission from Ref. [51]). B) Optical fluorescence images of adult human NSCs cultured on different PDMS substrates after 7 days of differentiation. Cells were stained with the neuronal specific marker Tuj-1 (red) and with DAPI for nuclear staining (blue). The size of the microchannels is indicated on top of each picture and the axis of the microchannels is indicated by the arrow.[49] Ca) SEM images of the BCP nanopore (NPS), microgroove (MPS), hierarchical (HPS) patterns and high magnification image of HPS; Cb) SEM images of hNSCs on flat substrate (FS), NPS, MPS and HPS (scale bar = 20 μm). The white arrowheads indicate sprouting of neurites from cell bodies across the microgroove patterns (scale bar = 1 μm) (Reprinted with permission from Ref. [40]). D) SEM images of nano- and microfibers (Da) and confocal microscopy images of immunostained neurofilament in NSCs after 2 days of culture (Db) on nanofibers (left) and microfibers (right); ×400 (Reprinted with the permission from Ref. [53]).

fiber diameters could promote specific differentiation fate.[46] Rat NSCs were cultured on electrospun fibers of random orientation in a growth medium which supports the differentiation into a mixed lineage of neurons, astrocytes and oligodendrocytes. While cells grown on fibers of an average diameter of 283 nm exhibited a threefold increase in oligodendrocyte differentiation when compared to the tissue culture polystyrene (TCPS) control, cells grown on fibers of 749 nm exhibited the highest fraction of neuronal differentiation among all substrates tested, as evidenced by the expression of the respective markers (Figure 2 A). These differences were confirmed by the morphology of the cells on the different fibrous substrates via

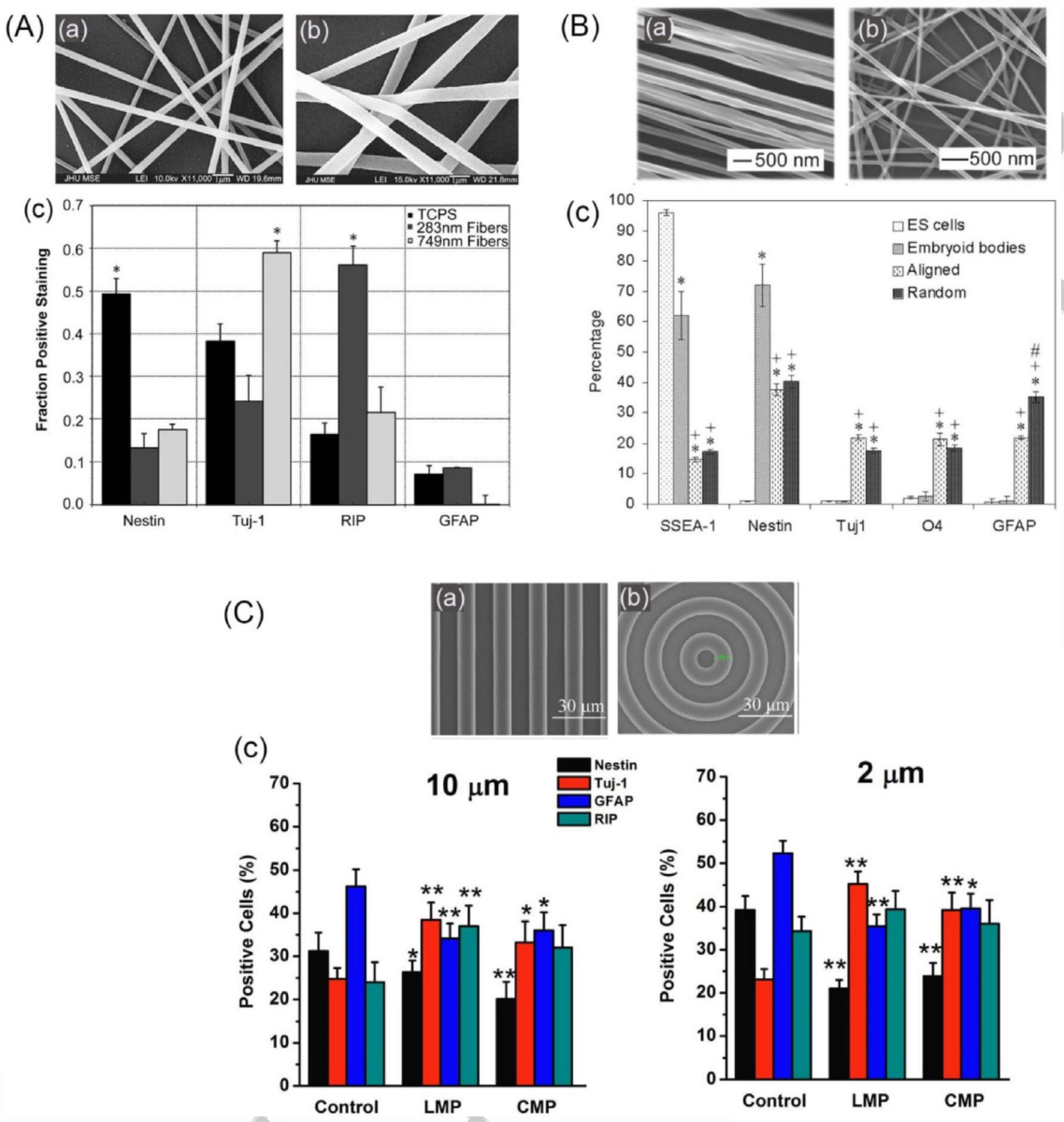

Figure 2. Tuning differentiation of stem cells into specific lineage. Aa–b) SEM images of randomly-oriented electrospun fibers of 283 (Aa) and 749 nm (Ab) diameter; Ac) Quantification of immunostaining results of rat NSCs cultured on various substrates in the presence of 1 mM retinoic acid and 1% FBS for 5 days (Reprinted with the permission from Ref. [46]). Ba–b) SEM images of parallel (Ba) and random (Bb) orientation PCL fibers; Bc) Cell phenotype analysis of RW4 EBs cultured on nanofibrous scaffolds for 14 days. The markers examined were SSEA-1 (for undifferentiated mouse ES cells), nestin (for neural precursors), Tuj1 (for neurons), O4 (for oligodendrocytes), and GFAP (for astrocytes) (Reprinted with permission from Ref. [44]). Ca–b) SEM images of the anisotropic linear (Ca) and cyclic (Cb) patterns. Cc) The graph shows the quantification of immunostaining results of the adult NSCs grown on the different substrates (of 2 μm and 10 μm width) in the presence of 1 mM RA and 2% FBS for 7 days (Reprinted with the permission from Ref. [51]).

SEM. When these cells were growing on fibers of a larger diameter (1452 nm) they showed lower viability.[46] Using submicron-sized PCL fibers (200–300 nm) of random orientation coated with graphene oxide (GO), Shah et al. reported the selective differentiation of NSCs into oligodendrocytes in a GO concentration-dependent way.[39] Their results support a role of GO-coating in the upregulation of these downstream molecules in the integrin signaling pathway. This preferential differentiation in oligodendrocytes may be associated with the size range of the fibers, which is morphologically close to the axonal diameter size.[39] However, in an older study it was shown that electrospun PCL random fibers of a diameter of 750 nm promoted the preferential differentiation of NSCs into oligodendrocytes as well.[45]

The effect of anisotropy■■OK?■■ on differentiation has been also investigated with the continuous anisotropic topographies of grooved substrates. In these studies, the groove/grating width seems to be a critical parameter for the differentiation fate of SCs. Linear or circular grooves of two different widths (10 and 2 μm) made of silicon showed that adult NSCs exhibited an increased and a decreased differentiation towards neurons and astrocytes, respectively, compared to the flat. This

response was more obvious on the smaller width (i.e. 2 μm) (Figure 2C).[51] The importance of grooved topography with emphasis on smaller widths on neuronal differentiation was also shown by Yang et al. Using PLGA grooved substrates of groove:ridge ratio 1:1 of three different widths (400, 800 and 5000 nm) and a proper surface coating consisting of DOPA, PLLA and fibronectin, they showed an enhanced differentiation in the presence of neurotrophic medium compared to that on the flat substrates. The effect was more striking on the nanopatterns (i.e. 400 and 800 nm).[55] This enhancement on neuronal differentiation on the patterns compared to the flat was less visible on the spontaneous differentiation conditions. Thus, the authors suggest a synergistic effect of biophysical (topography) and biochemical cues (growth medium and surface chemistry) on NSC differentiation.

In an attempt to investigate whether fiber orientation or fiber diameter has a greater impact on the differentiation fate of NSCs, some studies compared the SC growth and differentiation on randomly and parallel-oriented polymeric fibers. Specifically, Yang et al. used PLLA nanofibers (diameter: 250 nm) and microfibers (diameter: 1250 nm) of parallel and random orientation. They showed increased differentiation (i.e. in terms of number of differentiated cells and neurite length) of cerebellar stem cells into neural lineage when these were grown on nanofibers compared to the case where grown on the microfibers, independent of the fiber orientation. These results suggest that NSC differentiation depended on the fiber dimension and not on the fiber alignment which influenced neurite outgrowth and cell morphology.[53] However, the effect of fiber orientation over fiber diameter on the differentiation fate of SCs is not yet clear. For example, the study of Lim et al. emphasizes the role of anisotropy over fibrous dimension on neuronal differentiation. Using submicron-diameter PCL fibers (260,480 and 930 nm) of parallel or random orientation, they showed that upon induction of differentiation with RA a higher fraction of a NSCs on aligned fibers exhibited markers of neuronal differentiation as compared with NSCs on random fiber or unpatterned surfaces.[56] In another study, Xie et al. compared the differentiation response of EBs from ESCs on random and aligned PCL fibers of 250 nm diameter. Aligned nanofiber substrates could enhance the differentiation of ES cells into neurons and oligodendrocytes, but discouraged the differentiation into astrocytes. The opposite response was observed on the random fibers, suggesting the importance of anisotropy (Figure 2B).[44] Perhaps these differences among the various studies could be attributed to the stem cell source (e.g. in terms of developmental age, etc.). Future studies are envisaged to shed light on this controversial response/effect.

Given that neurons are electrically responsive cells, there is increasing interest in substrates which combine topographical cues with electrical cues. Accordingly, conductive materials, such as carbon nanotubes (CNTs), have been combined with medically approved polymers to form highly conductive composites. CNTs have been either blended with the polymers before processing[43] or incorporated at a post-processing step.[57] Interestingly, the studies show an increased neuronal differentiation on these composites compared to their counterparts (i.e. without the conductive component) even without electrical stimulation. Accordingly, Landers et al. developed composites of electrospun poly(lactic-co-glycolic acid) (PLGA) fibers with single-walled carbon nanotubes (SWNTs), and investigated the ability of these substrates to enhance differentiation of induced pluripotent stem cell (iPSC)-derived NSCs. Increased neuronal differentiation on the SWNT-PLGA composites compared to the 2D control (PLGA thin film glass coverslips) was demonstrated.[57] Interestingly, the kinetics of neuronal differentiation was further enhanced when electrical stimulation was applied. This effect suggests that the stimulation activates a pathway that induces differences in secondary remodeling phenomena, which results in longer term effects on neuronal differentiation. They also confirmed the functionality of the differentiated neurons with sypaptophysin (i.e. a synaptic vesicle protein) immunocytochemistry and calcium imaging, where electrically active cells are defined as those that show an increase in fluorescence due to calcium influx in response to an external electrical stimulation.[57] Using aligned nanofiber electrospun scaffolds composed of PLLA blended with either single- or multi-walled carbon-nanotubes, Kabiri et al. reported a significant upregulation of neuronal markers of ESCs on the composite fibers compared to the pure PLLA ones.[43]

An interesting question is whether the topography, that is, without the presence of a differentiation agent, could promote NSCs and ESCs differentiation. In this context, studies with continuous topographies of alternating grooves and ridges report a significant up-regulation of neuronal marker, suggesting the differentiation towards neuronal lineage even in the absence of the proper differentiation agent. More specifically, Lee et al. cultured hESCs onto nanoscaled polyurethane acrylate grooves (width: 350 nm, spacing: 350 nm) and showed that nanotopography could effectively induce the differentiation of the hESCs preferentially into neuronal lineage but not to neuroglial after 5 days without the use of any differentiation agents. Although hESCs on both the patterned and the unpatterned control substrate expressed nestin, which is indicative for differentiation, only the hESCs on the 350 nm ridge/groove pattern arrays stained positive for Tuj1, and negative for brachyury (mesoderm marker) and Pdx1 (endoderm marker), compared with the hESCs on the flat surface control (Figure 3A).[52] Ankam et al. investigated the role of various topographical cues, such as continuous anisotropic cues of micro and nano-sized gratings and discontinuous such as isotropic pillars—patterned on PDMS- on the differentiation of hESCs.[48] Following a "direct differentiation'' protocol, in which small clumps of undifferentiated hESCs were cultured directly without going through the stage of embryoid body formation for 7 days, they showed that the anisotropic patterns of gratings independent of scale promoted neuronal (TuJ1 +) differentiation of hESCs, compared to the isotropic patterns or the flat that promoted the differentiation towards a neuroglial lineage (GFAP +). Among the different gratings, it was shown that cells on the nano-scale gratings (of 250 nm width, spacing and height) as compared to the three micro-gratings (w:s:h = 2:2:2,

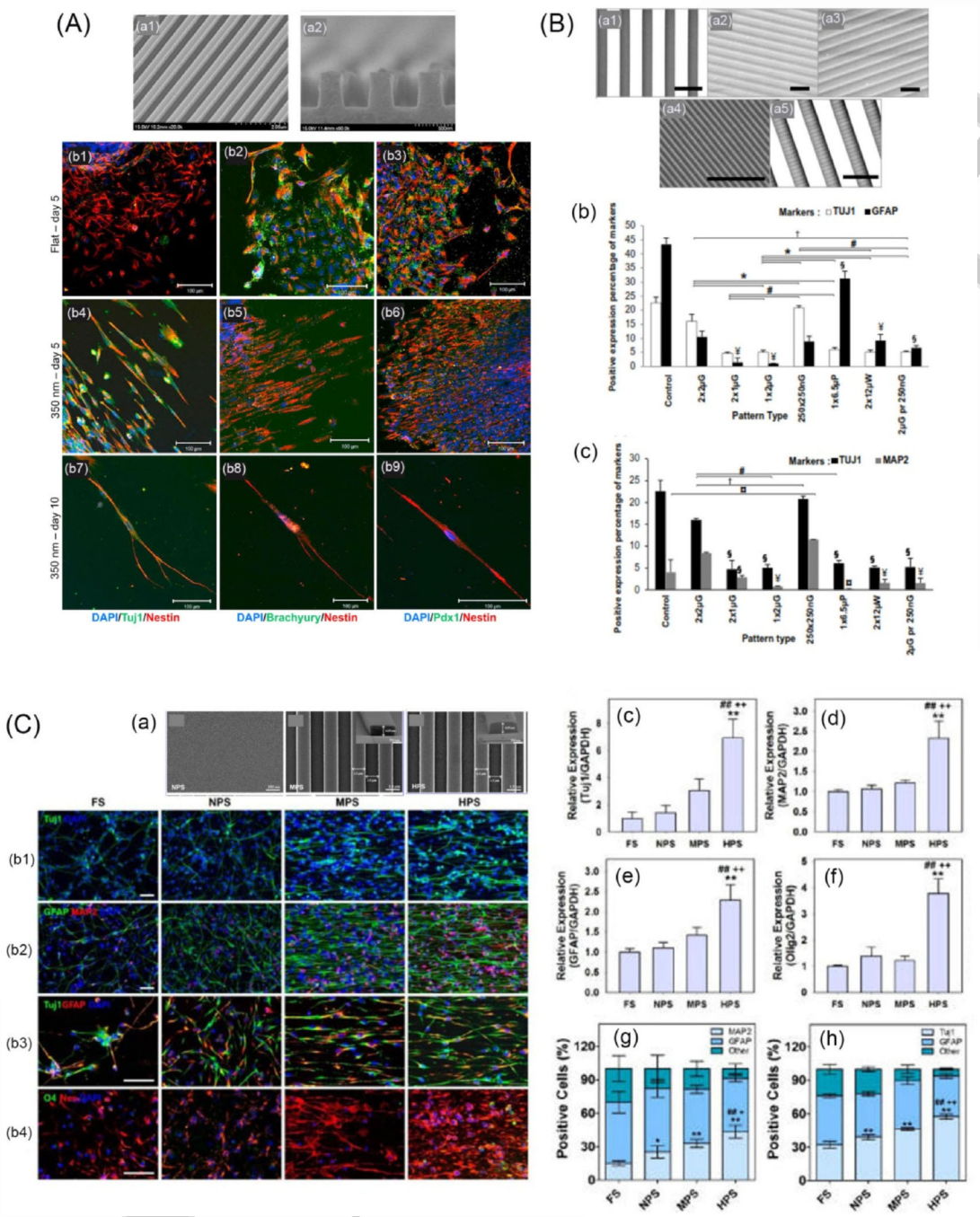

Figure 3. Effect of continuous anisotropic topographies on differentiation of stem cells into neurons without the use of differentiation agents. A) SEM images [overview (Aa1) and cross-section view (Aa2) of PUA 350 nm ridge/groove pattern arrays]. Ab) Neural differentiation of hESCs cultured on the PUA flat surface for five days (Ab1-3) and on the 350-nm ridge/groove pattern arrays [for five (Ab4-6) and ten (Ab7-9) days]; hESCs were immunostained for DAPI, Tuj1, Brachyury, PDX1 and Nestin (Reprinted with the permission from Ref. [52]). Ba) SEM images of the PDMS micro- & nanoscale grooved patterns of varying dimensions (Scale bar: 5 μm). Bb–c) Graphs showing the percentage of H1-derived neuronal cells (Tuj1$^+$), mature neuronal cells (MAP2$^+$) and glial cells (GFAP$^+$) on each pattern after seven days of differentiation (Reprinted with permission from Ref. [48]). Ca) SEM images of the nanopore (NPS), microgroove (MPS) and hierarchical (HPS) patterns and high magnification image of the HPS. Cb) Immunofluorescent staining of hNSCs differentiated on each substrate for neuronal (Tuj1 and MAP2), astrocyte (GFAP), oligodendrocyte (O4) and undifferentiated NSC (nestin) markers (scale bars = 50 μm); qRT-PCR analysis to measure the expression of the genes for Tuj1 (Cc), MAP2 (Cd), GFAP (Ce) and Olig2 (Cf) in hNSCs grown on each substrate. Relative proportion of MAP2$^+$ or GFAP$^+$ cells (Cg) and Tuj1$^+$ or GFAP$^+$ cells (Ch) on each substrate (Reprinted with permission from Ref. [40]).

2:1:0.12 and 1:2:0.08 μm), expressed more of the mature neuronal marker, MAP2 (Figure 3 B).[48]

The preferential differentiation of NSCs into neuronal lineage was also shown with a hierarchical topographical model consisting of nano-pored (pore diameter: 10 nm) grooves (of 1.5 μm width and spacing). When hNSCs were cultured under spontaneous differentiation medium conditions, differentiation into neuronal (Tuj1 + and MAP2 +) and astrocyte (GFAP +) line-

age was enhanced on the hierarchical patterned substrates (HPS) compared with the flat or single-type patterned substrates (micro- or nanopatterned substrates) with an increased ratio of the Tuj1+ cells relative to GFAP+ cells (Figure 3C). These results suggest that hierarchical patterns directed the fate of differentiated hNSCs to a neuronal rather than a glial lineage. This study was one of the first where the functionality of the neurons was investigated with the use of whole cell patch clamp, and it was confirmed that neurons differentiated from hNSCs on the HPS were electrophysiologically active after 5 days in culture exhibiting sodium currents and action potentials. This study proposes that nanopattern at the dimensions of integrin receptors/molecules can have a synergistic effect on directing the differentiation fate of NSCs.[40]

Apart from NSCs and ESCs, bone-marrow-derived stem cells (BMSCs) have been studied for their differentiation towards neurons. More specifically, BMSCs were cultured on three different micropatterned nanoridges of 24 nm of varying width/spacing (80/40, 40/30 and 30/20 μm) made of hydrogenated amorphous carbon (a-C:H). Although stem cells underwent neurogenesis in the presence of chemical induction medium (BDNF), as evaluated by the expression of Tuj1 and the levels of released nitric oxide, stem cells on the 40/30 μm were able to differentiate into neuronal lineage even in the absence of the BDNF, suggesting the implication of cell signaling associated with specific mechanical features of the patterned substrate.[37] Human bone marrow-derived mesenchymal stem cells (MSCs) grown on PDMS nanogratings of 350 nm depth and 350 nm width expressed early neuronal markers, such as MAP-2, with but also without the treatment of a chemical induction agent (i.e. RA).[38] Using comparatively micro-scale grating (of 1 and 10 μm width) and unpatterned PDMS, they showed that nanopattern had a more significant effect in stem cell behavior compared to the micropattern and the flat, in terms of differentiation and proliferation.[38] However, it has to be stressed that, although neuronal marker expression indicates differentiation of MSCs into a neuronal lineage, their functional role must be confirmed as well, since this behavior represents a transdifferentiation, as Turner and Dalby in their remarkable review emphasize.[2]

2.2. The Effect of Discontinuous Topographies on Neural Stem Cells

In contrast to continuous topographies, there are only a few reports on the effect of discontinuous topographies on NSCs. According to these studies, it is generally suggested that discontinuous isotropic topographies influence differentiation fate towards glial lineage rather than neuronal lineage, which is the case in continuous anisotropies. Qi et al. developed silicon linear-, circular- and dot-shaped micropattern (LMP, CMP and DMP, respectively) of 4 μm depth and of two different widths (10 μm and 2 μm); adult NSCs were cultured on them in the presence of RA and FBS.[51] Although cells on the continuous anisotropic topographies (LMP and CMP) were highly aligned along the axis (s. Section 2.1), cells on the DMP showed no preferred orientation and alignment (Figure 4Ab). Regarding their differentiation, cells on DMP showed an decreased differentiation into a neuronal lineage compared to the LMP and CMP, suggesting that the polarity of cells may influence the differentiation fate.[51] This trend was more striking for the smaller feature sizes (Figure 4Ac).[51] Ankam et al. investigated the role of various topographical cues on the differentiation of ESCs. They cultured hESCs on continuous anisotropic cues of gratings (s. Section 2.1) and discontinuous isotropic microscale-sized pillars (diameter: 1 μm; pitch: 6.5 μm and height: 1 μm) and wells (diameter: 2 μm; pitch: 12 μm; depth: 2 μm) patterned on PDMS. Although cells had been treated with differentiation medium that enhanced the differentiation into a mixed lineage of neurons, astrocytes, and oligodendrocytes, discontinuous isotropic patterns of pillars and wells promoted the glial rather than the neuronal differentiation of hESCs, which was the opposite response compared with that on the continuous anisotropic topographies. Gene expression analysis revealed a differential expression of oligondendrocyte- and astrocyte-specific genes on the two discontinuous patterns, showing that more hESCs differentiated into oligodendrocytes and astrocytes on pillars and on wells, respectively (Figure 4B).[48]

The differentiation of NSCs derived from the cerebral cortex of embryonic mice was also demonstrated using micro-patterned polymer membranes, also known as honeycomb (HC) films, which were fabricated through a condensation and evaporation process where the pore size can be precisely controlled. The membranes had pores of 3 to 15 μm size. The number of differentiated cells increased with increasing pore size. Membranes with a pore size of 3 and 5 μm suppressed the differentiation of NSCs.[59] Especially in the case of 3 μm, where the highest suppression was recorded, NSCs were trapped on the pore of the HC film, providing a small adhesion area.

Extending the study of the effect of discontinuous topography to nano-scaled discontinuous topographies is highly envisaged, given that stem cells of other origin are shown to be critically responsive to these. Indeed, specific nanoscale topographical patterns were shown to stimulate MSCs osteogenic differentiation to produce bone mineral in vitro in the absence of osteogenic supplements,[60] while other nanopatterns helped MSCs to maintain their stem cell multipotency.[61]

2.3. The Effect of Random Topographies on Neural Stem Cells

Random topographies with nano-sized features have been shown to favor the selective differentiation towards a specific fate (neuronal or glial) depending on the topographical model. Blumenthal et al. used assembly of monodispersed silica colloids of increasing size in an attempt to mimic the topography of the level of receptor clusters up to ECM features.[62] They showed that there was a favored regime ($R_q = 16–32$ nm) upon which telencephalic NSCs spontaneously differentiated into neurons in the absence of exogenous soluble signals. This differentiation response was the same even under exogenous signals that favor astrocytic differentiation.[62]

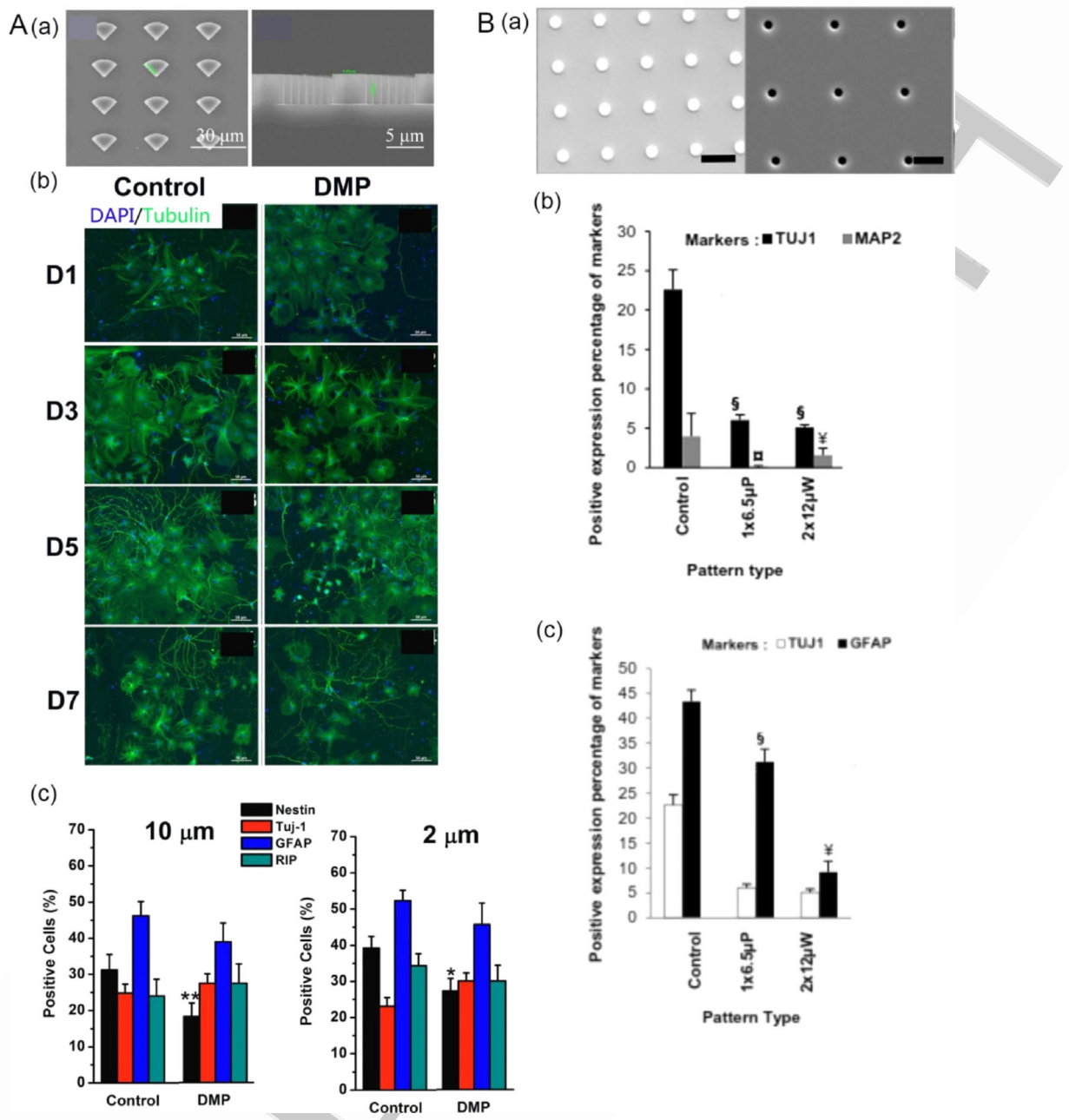

Figure 4. Effect of discontinuous topographies on NSCs: Aa) Top-view (left) and cross-section (right) SEM images of the dot-shaped (DMP) silicon micro-patterns. Ab) Fluorescence microscopy images of the NSCs on the control and the DMP substrates for different days from 1–7 (D1-D7). Ac) The graph shows the quantification of immunostaining results of the adult NSCs grown on the different substrates (of 2 μm and 10 μm width) in the presence of 1 mM RA and 2% FBS for 7 days [Reprinted with permission from [51]. Ba) SEM images of the: (left) 1 μm pillar width 6.5 μm pitch and 1 μm height ("μP"), (right) 2 μm wells with 12 μm pitch and 2 μm height ('μW') (Scale bar: 5 μm). Bb) H1-derived neuronal cells (Tuj1$^+$) and mature neuronal cells (MAP2$^+$) on each pattern after 7 days of differentiation. Bc) H1-derived neuronal cells (Tuj1$^+$) and glial cells (GFAP$^+$) on each pattern after seven days of differentiation [Reprinted with permission from Ref. [48]].

Mou et al. showed that rat NSCs on a nanoporous titanium oxide (TiO_2) surface (pore: 200–500 nm) showed a preferential differentiation into astrocyte and less into neuronal lineage, which was the case for the flat TiO_2 and tissue culture plastic. This effect was independent of surface chemistry; PDMS replicas of the patterns showed similar results. Furthermore, the morphology of the astrocytes was different; NSCs on porous TiO_2 differentiated into fibrous astrocytes, while NSCs on TCP and flat TiO_2 differentiated into protoplasmic astrocytes.[63] Interestingly, porous TiO_2 showed a remarkably higher protein adsorption, measured by BCA assay, compared to the flat TiO_2, although the two substrates did not differ in terms of wettability.

Human NSCs on monolayers of oxygen-terminated nanodiamonds, exhibiting a roughness of R_q: 3.84 nm, showed a good cell attachment, which was comparable to that on TCPS with the same roughness (R_q: 3.74 nm).[64] However, the more hydrophobic H-terminated nanodiamonds could not support cell at-

tachment. The authors suggest that the different surface chemistry mediates different binding of the protein laminin affecting in turn the cell response.

Using a novel approach, Solanki et al. developed a nanotopography-mediated reverse uptake (NanoRU) delivery platform to demonstrate the control of the differentiation fate of NSCs via siRNA delivery into cells.[65] The platform consists of a self-assembled silica nanoparticle (SiNP) monolayer coated with extracellular matrix proteins and the desired siRNA.[65] As a first step, they confirmed the nanotopography-mediated effect using siRNA against green fluorescent protein (GFP). Negatively-charged siRNA molecules and laminin condensed together on the positively-charged SiNPs. The NSCs were then seeded on these NanoRUs and the knockdown of GFP in the NSCs was imaged using a fluorescence microscope. By varying the dimension of the silica nanoparticles, ranging from 100–700 nm, the amount of the delivered siRNA varied, with the 100 nm exhibiting the best uptake. Using a siRNA against the transcription factor SOX9, which acts as a switch between neuronal and glial fate of NSCs, the authors showed the successful suppression of the SOX9 and the selective differentiation of NSCs into neurons.

3. The Effect of Topography on NSCs—An Insight into the Mechanisms

Although in the last years there is experimental evidence showing that NSCs respond to topographical cues by altering their shape and their functions, a mechanism responsible for this behavior is lacking. In general, cells recognize the physical and topographical characteristics of the surrounding extracellular milieu predominantly through the integrins, the cell surface receptors that bind to specific ECM motifs.[67] Integrins bind to ECM through a complex mechanism involving the formation of attachment points resulting in tension formation within the cell and at the same time transmitting information from the ECM inside the cell. Specifically, integrin activation and clustering leads to the assembly of focal complexes which mature into focal adhesions (FAs), which are multiprotein complexes that link the integrins to the actin filaments of the cytoskeleton. Recruitment of the actin-binding FA proteins, such as vinculin and paxilin, causes actin stress fiber formation and force transduction through the actin-myosin cytoskeletal network; thus, resulting in changes in cytoskeletal tension.[68] Accordingly, the FAs provide mechanical/physical links to the cell's contractile architecture and can directly result in changes in cytoskeletal organization, structure and finally cell shape.[69] Furthermore, FAs incoroporate the signalling proteins that initiate downstream biochemical signal cascades, including the activation of phosphorylation- and G-protein (like Rho-mediated pathways, for example, ROCK), which can lead to long-term changes in transcriptional regulation, cell proliferation and differentiation.[70] Thus, via feedback loops that connect cell adhesion, contractility and signalling, cells sense and respond to the physical properties of their surroundings. In accordance to this pathway, studies on the substrate-guided stem cell fate focus on the: 1) ECM-integrin interactions, 2) focal adhesion formation and ROCK signaling and 3) actin-myosin contractility.

In the case of NSCs, during the development of the CNS, the highly organized and temporally defined process of their migration from the stem cell niche to their differentiation to mature neurons depends heavily on cell–cell and cell–ECM interactions. NSCs within the developing and mature adult brain interact with ECM via integrins. Among the various integrin subunits, β1 integrins are suggested to provide NSC with the capacity to react to a dynamic "niche'' and to respond adequately by either preserving their stem cell state or by differentiating and migrating away to shape the developing cortex (reviewed in [71,72]). For example, β1 integrins are required for the formation of the radial glial scaffold upon migration.[73] Among these integrins, α5β1 and α6β1, which recognize the ECM proteins fibronectin and laminin, respectively, seem to play a critical role during CNS development.[71] It is speculated that differential ECM patterns acting on successive β1 integrin expression and in combination with differential growth availability modulate NSC proliferation and survival and differentiation in the developing cortex and the adult neurogenic compartments.[71]

Accordingly, topography can play a critical role in the way specific proteins deposit selectively onto the surface, which then influences the cell binding via the integrin activation.[74] A distinct protein adsorption was shown on hydrogen-terminated ultracrystalline nanodiamond films (H-UNCD) with grain morphology (average grain size: 5 nm; Figure 5 Ba). Specifically, these substrates showed increased fibronectin adsorption compared to the control PS. NSCs on these nano-diamond films exhibited spontaneous differentiation and increased β1 expression, compared to the control PS.[66] Functional-blocking antibody directed against integrin β1 subunit, which is correlated with fibronectin, inhibited neuronal differentiation of NSCs on the H-UNCD films, suggesting the involvement of integrin β1 in H-UNCD-mediated neuronal differentiation. Furthermore, NSCs on the nanodiamonds showed increased phosphorylation of FAK and Erk1/2 (Figure 5 Bi,j). However, the enhancement of Erk1/2 pathway was suppressed when treating with the MEK inhibitor U0126 (Figure 5 Bk). Together, these results suggest that fibronectin, which is selectively adsorbed on the nanodiamond topography, binds to integrin β1 and activates integrin signaling pathway resulting in tyrosine phosphorylation of FAK, and then elicits MEK/Erk signaling pathway.[66]

Integrin binding, F-actin reorganization, and focal adhesion assembly seem to be involved in the enhanced differentiation of hNSCs on a hierarchically patterned topographical model consisting of a nanopore-patterned micro-grooved topography (s. Figure 3 C).[40] Addition of β1-integrin antibodies disrupted adhesion and alignment of hNSCs along the patterns. Specifically, it eliminated the beneficial effects of the hierarchical patterns compared to the other two patterns (i.e. nano-pored pattern and micro-grooved pattern) in terms of focal adhesion formation (Figure 5 A) and enhanced differentiation of hNSCs into neurons and astrocytes. This was expressed by the decrease of the respective protein markers and the morphological alterations of the cells. The same effect was observed after treat-

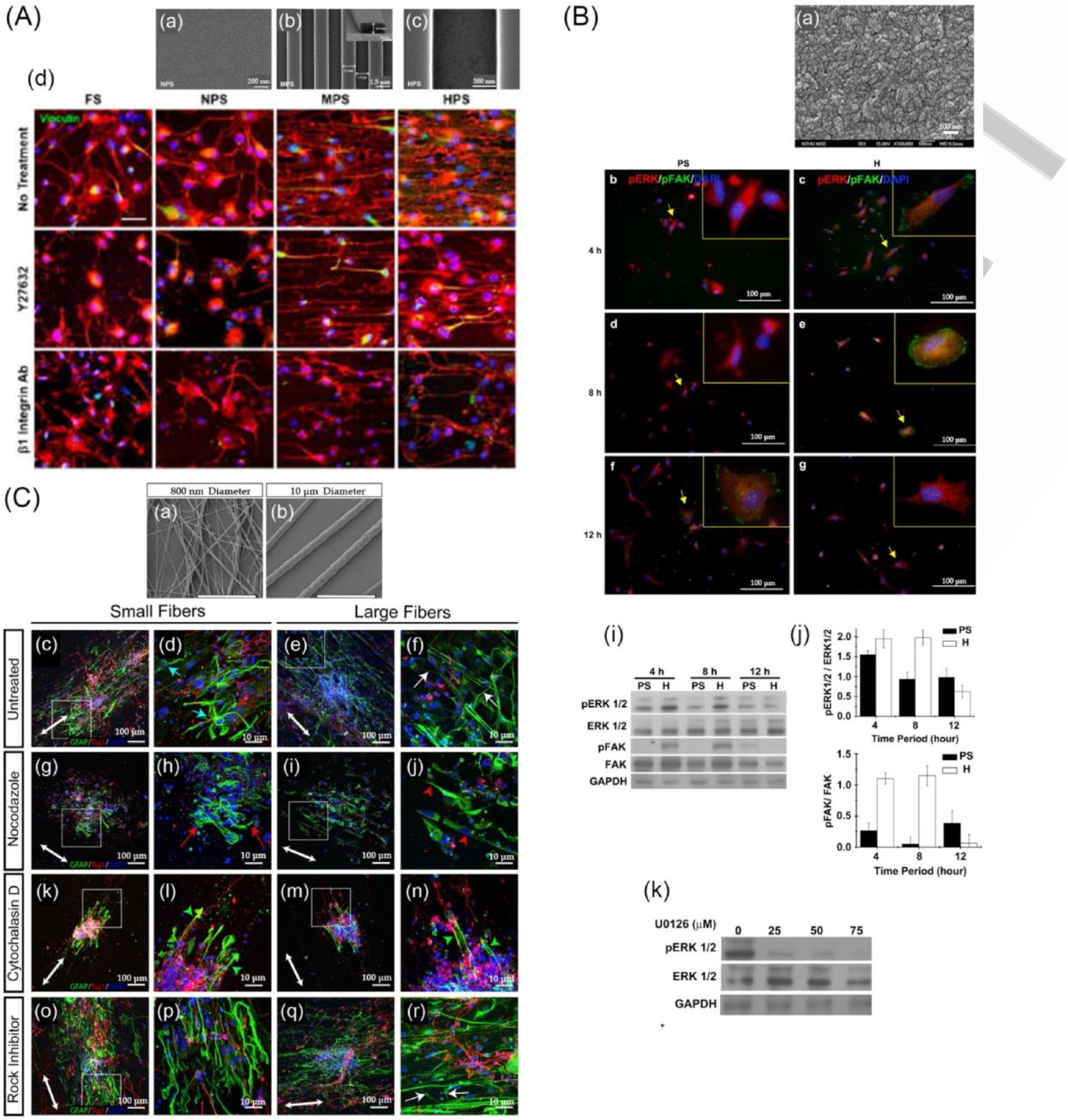

Figure 5. Investigating the mechanism of the effect of topographical cues on NSCs functions/responses. Aa–c) SEM images of: Aa) nanopore (NPS), Ab) microgroove (MPS), Ac) hierarchical (HPS) patterns, and high-magnification image of hierarchical patterns [scale bars: 200 nm (a), 1.5 μm (b), 500 nm (c)]. Ad) Inhibition of focal adhesion, alignment of the cytoskeleton, and differentiation of hNSCs by treatments with the ROCK inhibitor (Y27632) and β1-integrin antibodies (1 day in culture). Staining of focal adhesion protein (vinculin) and cytoskeleton (F-actin) and of hNSCs on each substrate with or without treatment with Y27632 and β1-integrin antibodies (scale bars = 50 μm). Cell nuclei were counterstained with DAPI (Reprinted with the permission from Ref. [40]). Ba) SEM image of H-UNCD films (H). Bb–g) Immunofluorescence triple labeling show staining patterns of Erk (red), Fak (green) and DAPI (blue) on NSCs at three different time points. Bi) Time course of Erk1/2 and Fak in NSCs incubated on HUNCD films (H). Bj) The ratio of phosphorylated ERK1/2 to total ERK1/2 and phosphorylated FAK to total FAK, determined by band densitometry analysis. Bk) Western blots were performed with anti-phosphorylated Erk1/2 and anti-Erk1/2 for NSCs cultured on H-UNCD films in the regular medium for 8 h followed by treatment with U0126 with different concentrations. GAPDH was used as an internal control (Reprinted with the permission from Ref. [66]). Ca–b) SEM images of the electrospun fiber mats. Cc–r) Mouse E13 neural stem cells grown onto small (two left columns) and large (two right panels) electrospun PCL fiber mats coated with laminin and treated with inhibitors of cytoskeletal polymerization. Cultures were incubated for ten days and then fixed and stained with GFAP (green), Tuj1 (red), and DAPI (blue); scale bar: 100 μm in (c), (e), (g), (i), (k), (m), (o), (q); 10 μm in (d), (f), (h), (j), (l), (n), (p), (r) (Reprinted with the permission from Ref. [25].

ment with Y27632, a ROCK inhibitor. Both treatments decreased vinculin-expressed cell adhesion, suggesting that β integrin binding and ROCK pathway are critical for focal adhesion of hNSCs on the patterned substrates (Figure 5 Ad).[40] These data emphasize the importance of β1 integrin-mediated binding and ROCK-mediated intracellular signaling pathways

for the promotion of focal adhesion formation, FAK pathway activation, and, in turn, the enhanced differentiation of hNSCs on the specific hierarchical topographical model. This may suggest potential mechanotransduction mechanisms of hNSC differentiation enhanced by hierarchical patterns.[40] In total, this study shows up the importance of hierarchical topography which can synergistically enhance the differentiation of human NSCs (hNSCs) by simultaneously providing microscale and nanoscale spatial controls to enhance the alignment of the cytoskeleton and the formation of focal adhesions, and paves the way for novel designs.

The breakthrough study of Czeisler et al. brings evidence on the importance of topography on regulating the cell–ECM interactions.[25] Inspired by neuroanatomical analysis on the VZ/SVZ and ependymal surface of human embryonic brains performed by the group, the researchers designed two types of electrospun fibrous matrices: fibers of 8.8 μm (large fibers) mimicking blood vessel topography and fibers of 0.86 μm (small fibers) mimicking the topography of the processes of radial glial (Figure 5 Ca-b). Study of the migration and differentiation of NSCs using the neurosphere model revealed differential migratory and morphological responses of the NSCs on the two patterns. Specifically, smaller-fiber topography, in both the poly-D-lysine (PDL)- and PDL/laminin-treated conditions, supported cell migration at day 10; individual cells showed alignment to the fiber mats. Large-fiber topography without laminin prevented cell migration, but this anti-migrating response was partially reversed by treatment with ROCK inhibitor.[25] This observation was supported by the documented inhibitory role of the Rho-associated kinase on the neoplastic astrocyte migration on vessels.[75] These results emphasize distinct cell-ECM interactions that are regulated by topography. Regarding cell morphology, cells on the small fibers were mainly of two astrocyte populations, that is, with fibrous/bipolar morphology and with multipolar morphologies (Figure 5 Cc-d), while cells on the large fibers showed predominantly fibrous/bipolar morphology (Figure 5 Ce-f). To investigate the role of cytoskeleton on the cell morphology, the researchers treated the neurospheres on the laminin-coated fibrous patterns with various cytoskeletal inhibitors, including nocodazole (to inhibit microtubules), cytochalasin D (to inhibit actin) and Y-27632 (to inhibit Rho-associated protein kinase). Remarkably, treatment of the neurospheres with cytoskeletal inhibitors induced subtle changes in cellular morphology in the case of the small fibers (Figure 5 Cg–h,k-l), but marked changes in the case of the large fibers (Figure 5 Ci-j,m-n). These results imply that cell morphology has different requirements on cytoskeletal proteins depending on the topographical environment encountered by the cell. Together these findings suggest that ECM-induced cell responses during development are modulated by the surface topography.[25]

In parallel with the effect on alignment and morphology, the effect of topography on preferential differentiation is critical. To investigate the mechanisms of selective differentiation of NSCs into neurogenic lineage on aligned submicron fibrous patterns, Lim et al. used PCL fibers of submicron diameters (i.e. 260, 480 and 930 nm) and studied two hypotheses.[56] According to the first hypothesis, the aligned fibrous topography was favorable to the attachment and survival of neuronal progenitors and conversely unfavorable to non-neuronal cell types. Indeed, aNSCs on culture dishes were treated with IGF/noggin and differentiated into oligodendrocytes, but showed decreased survival and attachement when replated on the fibrous patterns. On the contrary, NSCs treated with RA and differentiated into neuronal lineage, showed better attachment on the fibrous patterns compared with the planar when replating. According to the second hypothesis, the fiber topography resulted in cytoskeletal rearrangements and subsequently leading to changes in intracellular signaling activation. In the absence of any additional biochemical cues, NSCs responded to parallel fiber topography with an increase in canonical Wnt signaling; this was further potentiated by RA treatment. The implication of canonical b-catenin/Wnt signaling pathway in neurogenesis in both embryonic and adult neural precursor cells is well reported.[76,77] These findings suggest that substrate topography can affect changes in gene expression (e.g. expression of cell differentiation markers) via cytoskeletal elongation. Together, these findings suggest a mechanism by which morphological control of stem cells operates in concert with biochemical cues for cell fate determination.[56]

Regarding the pluripotent ESCs, the studies presented in Chapter 2 were focused on the regulation of the neurogenic differentiation of ESCs by topography/specific patterns. Furthermore, the mechanism by which topography mediates the regulation of ESCs' self-renewal versus differentiation by cell adhesion and shape/spreading is very important. In the study of Kong et al. polystyrene nanopillars in two different configurations- hexagonal and honeycomb—with various spacing ranging from 50–300 nm have been used for the culture of hESCs in different culture media.[78] A reduced number of focal adhesions compared to the flat substrates was reported, as detected by the expression of paxillin and morphological study via SEM. Immunostaining for Oct4 showed that, while hESCs on the flat began to down-regulate the Oct4 expression without bFGF supplementation, hESCs on the nanostructured substrates did maintain the expression of Oct4. These data suggest that disruption of focal adhesions may help maintain the expression of Oct4 without bFGF supplementation.[78]

In parallel to the effect on integrins, cytoskeleton, and FAs, topography may have an impact on intercellular interactions, which in turn may influence SC differentiation. Studies focusing on this investigate the alteration in expression of specific cell-cell proteins, like E-cadherin. Chen et al. showed that stochastic nanoroughness (R: 75–150 nm) imprinted/patterned on glass influenced adhesion, spreading, and self-renewal of hESCs.[79] A differential expression pattern of FA markers on nanorough compared to smooth glass was reported. More specifically, vinculin-containing FAs of the self-renewing, undifferentiated, ESCs (Oct3/4+) formed primarily on the periphery of the cells, but distributed randomly throughout the entire cell spread area on the nanorough surface, suggesting that the nanotopography may significantly impact the molecular arrangement, formation and distribution of FAs in hESCs. Staining for E-cadherin showed a concentrated expression on the

cell-cell contacts in the case of the undifferentiated cells but had a decreased expression in the spontaneously differentiated cells (Oct3/4-) on the smooth glass. Interestingly, E-cadherin expression was downregulated in cells at both states on the nanorough regions, suggesting a disruption of the intercellular adhesion of hESCs. These results suggest that the local random nanotopographical cues can directly influence the FA formation and E-cadherin-regulated intercellular adhesion which may in turn influence the cellular response of self-renewal of the hESCs.[79]

Beyond its effect on integrin activation and intercellular communication, topography may influence stem-cell functions via other mechanisms, like triggering mechanosensitive ion channels or through secondary effects, such as alterations in the effective stiffness of the substrate.[1] However, these remain still largely unexplored.

4. Conclusion

New types of cell culture platforms with various topographical patterns at the micro- and the nanoscale have been used to study (in vitro) the effect of surface topography on NSC and ESC growth and differentiation into neuronal and/or neuroglial lineage. Continuous topographies in the form of 1) alternating grooves/ridges of subcellular and cellular width and 2) parallel aligned fibers of subcellular diameter were shown to strongly promote neurite guidance and orientation along groove or fiber axis, respectively. At the same time, the effect of topography seems to be critical for the differentiation fate of NSCs or ESCs. Anisotropic topographies of grooved substrates enhanced NSCs or ESCs differentiation towards neuronal over neuroglial fate, in both neurogenic and spontaneous differentiation medium. In the case of the fibers, it is less clear whether the fiber diameter or the fiber orientation (i.e. aligned vs. random) has a greater impact on the differentiation fate of NSCs; future studies are needed to investigate this response.

Discontinuous topographies in the form of circular, dot or pillar patterns, with diameters and inter-feature spacing at subcellular to cellular scale (e.g. 2 to 15 μm), influenced differentiation fate towards glial rather than neuronal lineage. Extending the study of the effect of discontinuous topography to nanoscale discontinuous topographies is highly envisaged, given that stem cells of other origin (i.e. MSCs) were shown to be critically responsive to these. Random topographies with nano-sized features favoured selective differentiation of NSCs towards a specific fate (neuronal or glial) depending on the topographical model.

Regarding the underlying mechanisms of topography sensing, studies have focused on ECM-integrin interactions, focal adhesion formation, and ROCK signalling, as well as cytoskeletal rearrangements. Topography is suggested to play a role in selective protein adsorption which influences the integrin activation (such as β1), but also to substrate selectivity for survival of specific cell populations. Besides this, surface topography is suggested to regulate the ECM-induced cell responses during development. Further studies are required to provide a broader insight into such mechanisms and contribute towards the understanding of NSC growth and differentiation during development with ultimate implementation in tissue engineering research.

Conflict of interest

The authors declare no conflict of interest.

Keywords: differentiation · micro-/nano-fabrication · neural stem cells · orientation · topography

[1] F. Guilak, D. M. Cohen, B. T. Estes, J. M. Gimble, W. Liedtke, C. S. Chen, *Cell Stem Cell* **2009**, *5*, 17 – 26.
[2] L.-A. Turner, M. J. Dalby, *Biomater. Sci.* **2014**, *2*, 1574 – 1594.
[3] M. F. Griffin, P. E. Butler, A. M. Seifalian, D. M. Kalaskar, *World J. Stem Cells.* **2015**, *7*, 37 – 50.
[4] L. De Filippis, E. Binda, *Stem Cells Transl. Med.* **2012**, *1*, 298 – 308.
[5] C. G. Gross, *Nat. Rev. Neurosci.* **2000**, *1*, 67 – 73.
[6] H. G. Kuhn, H. Dickinson-Anson, F. H. Gage, *J. Neurosci.* **1996**, *16*, 2027 – 2033.
[7] B. A. Reynolds, S. Weiss, *Science* **1992**, *255*, 1707 – 1710.
[8] A. Achilleos, P. A. Trainor, *Cell Res.* **2012**, *22*, 288 – 304.
[9] Q. Shen, Y. Wang, E. Kokovay, G. Lin, S. M. Chuang, S. K. Goderie, B. Roysam, S. Temple, *Cell Stem Cell* **2008**, *3*, 289 – 300.
[10] D. E. Discher, D. J. Mooney, P. W. Zandstra, *Science* **2009**, *324*, 1673 – 1677.
[11] P. S. Eriksson, E. Perfilieva, T. Björk-Eriksson, A. M. Alborn, C. Nordborg, D. A. Peterson, F. H. Gage, *Nat. Med.* **1998**, *4*, 1313 – 1317.
[12] C. Lois, A. Alvarez-Buylla, *Proc. Natl. Acad. Sci. USA* **1993**, *90*, 2074 – 2077.
[13] M. S. Kaplan, J. W. Hinds, *Science* **1977**, *197*, 1092 – 1094.
[14] B. Seri, D. G. Herrera, A. Gritti, S. Ferron, L. Collado, A. Vescovi, J. M. Garcia-Verdugo, A. Alvarez-Buylla, *Cereb. Cortex* **2006**, *16*, i103 – i111.
[15] A. Lee, J. D. Kessler, T.-A. Read, C. Kaiser, D. Corbeil, W. B. Huttner, J. E. Johnson, R. J. Wechsler-Reya, *Nat. Neurosci.* **2005**, *8*, 723 – 729.
[16] G. L. Ming, H. Song, *Neuron* **2011**, *70*, 687 – 702.
[17] S. W. Lane, D. A. Williams, F. M. Watt, *Nat. Biotechnol.* **2014**, *32*, 795 – 803.
[18] C. Regalado-Santiago, E. Juárez-Aguilar, J. D. Olivares-Hernández, E. Tamariz, *Stem Cells Int.* **2016**, 1513285.
[19] F. Gattazzo, A. Urciuolo, P. Bonaldo, *Biochim. Biophys. Acta Gen. Subj.* **2014**, *1840*, 2506 – 2519.
[20] F. Doetsch, J. García-Verdugo, A. Alvarez-Buylla, *J. Neurosci.* **1997**, *17*, 5046 – 5061.
[21] F. Doetsch, *Curr. Opin. Genet. Dev.* **2003**, *13*, 543 – 550.
[22] L. Bozoyan, J. Khlghatyan, A. Saghatelyan, *J. Neurosci.* **2012**, *32*, 1687 – 1704.
[23] C. S. Bjornsson, M. Apostolopoulou, Y. Tian, S. Temple, *Dev. Cell* **2015**, *32*, 435 – 446.
[24] C. Lee, J. Hu, S. Ralls, T. Kitamura, Y. P. Loh, Y. Yang, Y. S. Mukouyama, S. Ahn, *PLoS One* **2012**, *7*, e50501.
[25] C. Czeisler, A. Short, T. Nelson, P. Gygli, C. Ortiz, F. P. Catacutan, B. Stocker, J. Cronin, J. Lannutti, J. Winter, J. J. Otero, *J. Comp. Neurol.* **2016**, *524*, Spc1.
[26] A. Wade, A. McKinney, J. J. Phillips, *Biochim. Biophys. Acta Gen. Subj.* **2014**, *1840*, 2520 – 2525.
[27] A. Purushothaman, K. Sugahara, A. Faissner, *J. Biol. Chem.* **2012**, *287*, 2935 – 2942.
[28] M. Karus, B. Denecke, C. French-Constant, S. Wiese, A. Faissner, *Development* **2011**, *138*, 5321 – 5331.
[29] E. Bazán, F. J. Alonso, C. Redondo, M. A. López-Toledano, J. M. Alfaro, D. Reimers, A. Herranz, C. L. Paíno, A. B. Serrano, N. Cobacho, E. Caso, M. V. Lobo, *Histol. Histopathol.* **2004**, *19*, 1261 – 1275.
[30] S. Temple, *Nature* **2001**, *414*, 112 – 117.
[31] T. S. Jacques, J. B. Relvas, S. Nishimura, R. Pytela, G. M. Edwards, C. H. Streuli, C. Ffrench-Constant, *Development* **1998**, *125*, 3167 – 3177.
[32] L. S. Campos, *J. Neurosci. Res.* **2004**, *78*, 761 – 769.

[33] M. V. Lobo, F. J. Alonso, C. Redondo, M. A. López-Toledano, E. Caso, A. S. Herranz, C. L. Paíno, D. Reimers, E. Bazán, *J. Histochem. Cytochem.* **2003**, *51*, 89 – 103.
[34] H. I. Kornblum, *Stroke* **2007**, *38*, 810 – 816.
[35] N. L. Kennea, H. Mehmet, *J. Pathol.* **2002**, *197*, 536 – 550.
[36] V. Mattis, S. Svendsen, D. Sareen, C. Svendsen, Nature Neuroscience (Poster). **2010**.
[37] F. D'Angelo, I. Armentano, S. Mattioli, L. Crispoltoni, R. Tiribuzi, G. G. Cerulli, C. A. Palmerini, J. M. Kenny, S. Martino, A. Orlacchio, *Eur. Cells Mater.* **2010**, *20*, 231 – 244.
[38] E. K. Yim, S. W. Pang, K. W. Leong, *Exp. Cell Res.* **2007**, *313*, 1820 – 1829.
[39] S. Shah, P. T. Yin, T. M. Uehara, S. T. Chueng, L. Yang, K. B. Lee, *Adv. Mater.* **2014**, *26*, 3673 – 3680.
[40] K. Yang, H. Jung, H. R. Lee, J. S. Lee, S. R. Kim, K. Y. Song, E. Cheong, J. Bang, S. G. Im, S. W. Cho, *ACS Nano* **2014**, *8*, 7809 – 7822.
[41] K. Michalczyk, M. Ziman, *Histol. Histopathol.* **2005**, *20*, 665 – 671.
[42] A. Cheng, S. Wang, J. Cai, M. S. Rao, M. P. Mattson, *Dev. Biol.* **2003**, *258*, 319 – 333.
[43] M. Kabiri, M. Soleimani, I. Shabani, K. Futrega, N. Ghaemi, H. H. Ahvaz, E. Elahi, M. R. Doran, *Biotechnol. Lett.* **2012**, *34*, 1357 – 1365.
[44] J. Xie, S. M. Willerth, X. Li, M. R. Macewan, A. Rader, S. E. Sakiyama-Elbert, Y. Xia, *Biomaterials* **2009**, *30*, 354 – 362.
[45] D. R. Nisbet, L. M. Y. Yu, T. Zahir, J. S. Forsythe, M. S. Shoichet, *J. Biomater. Sci. Polym. Ed.* **2008**, *19*, 623 – 634.
[46] G. T. Christopherson, H. Song, H. Q. Mao, *Biomaterials* **2009**, *30*, 556 – 564.
[47] L. Qi, N. Li, R. Huang, Q. Song, L. Wang, Q. Zhang, R. Su, T. Kong, M. Tang, G. Cheng, *PLoS One* **2013**, *8*, e59022.
[48] S. Ankam, M. Suryana, L. Y. Chan, A. A. Moe, B. K. Teo, J. B. Law, M. P. Sheetz, H. Y. Low, E. K. Yim, *Acta Biomater.* **2013**, *9*, 4535 – 4545.
[49] A. Béduer, C. Vieu, F. Arnauduc, J. C. Sol, I. Loubinoux, L. Vaysse, *Biomaterials* **2012**, *33*, 504 – 514.
[50] C. Simitzi, A. Ranella, E. Stratakis, *Acta Biomater.* **2017**, *51*, 21 – 52.
[51] L. Qi, N. Li, R. Huang, Q. Song, L. Wang, Q. Zhang, R. Su, T. Kong, M. Tang, G. Cheng, *PLoS One* **2013**, *8*, e59022.■■same as ref. 47. Please check and replace or remove + renumber■■
[52] M. R. Lee, K. W. Kwon, H. Jung, H. N. Kim, K. Y. Suh, K. Kim, K. S. Kim, *Biomaterials* **2010**, *31*, 4360 – 4366.
[53] F. Yang, R. Murugan, S. Wang, S. Ramakrishna, *Biomaterials* **2005**, *26*, 2603 – 2610.
[54] Y. Yuan, P. Zhang, Y. Yang, X. Wang, X. Gu, *Biomaterials* **2004**, *25*, 4273 – 4278.
[55] K. Yang, E. Park, J. S. Lee, I. S. Kim, K. Hong, K. I. Park, S. W. Cho, H. S. Yang, *Macromol. Biosci.* **2015**, *15*, 1348 – 1356.
[56] S. H. Lim, X. Y. Liu, H. Song, K. J. Yarema, H. Q. Mao, *Biomaterials* **2010**, *31*, 9031 – 9039.
[57] J. Landers, J. T. Turner, G. Heden, A. L. Carlson, N. K. Bennett, P. V. Moghe, A. V. Neimark, *Adv. Healthcare Mater.* **2014**, *3*, 1745 – 1752.
[58] I. Sridharan, T. Kim, R. Wang, *Biochem. Biophys. Res. Commun.* **2009**, *381*, 508 – 512.
[59] A. Tsuruma, M. Tanaka, S. Yamamoto, M. Shimomura, *Colloids Surf. A* **2008**, *313*, 536 – 540.
[60] M. J. Dalby, N. Gadegaard, R. Tare, A. Andar, M. O. Riehle, P. Herzyk, C. D. W. Wilkinson, R. O. C. Oreffo, *Nat. Mater.* **2007**, *6*, 997 – 1003.
[61] R. J. McMurray, N. Gadegaard, P. M. Tsimbouri, K. V. Burgess, L. E. McNamara, R. Tare, K. Murawski, E. Kingham, R. O. Oreffo, M. J. Dalby, *Nat. Mater.* **2011**, *10*, 637 – 644.
[62] N. R. Blumenthal, O. Hermanson, B. Heimrich, V. P. Shastri, *Proc. Natl. Acad. Sci. USA* **2014**, *111*, 16124 – 16129.
[63] X. Mou, S. Wang, W. Guo, S. Ji, J. Qiu, D. Li, X. Zhang, J. Zhou, W. Tang, C. Wang, H. Liu, *Nanoscale* **2016**, *8*, 13186 – 13191.
[64] A. C. Taylor, C. H. González, B. S. Miller, R. J. Edgington, P. Ferretti, R. B. Jackman, *Sci. Rep.* **2017**, *7*, 7307.
[65] A. Solanki, S. Shah, P. T. Yin, K.-B. Lee, *Sci. Rep.* **2013**, *3*, 1553.
[66] Y.-C. Chen, D.-C. Lee, T.-Y. Tsai, C.-Y. Hsiao, J.-W. Liu, C.-Y. Kao, H.-K. Lin, H.-C. Chen, T. J. Palathinkal, W.-F. Pong, N.-H. Tai, I.-N. Lin, I.-M. Chiu, *Biomaterials* **2010**, *31*, 5575 – 5587.
[67] J. C. Adams, F. M. Watt, *Development* **1993**, *117*, 1183 – 1198.
[68] S. Vainio, U. Muller, *Cell* **1997**, *90*, 975 – 978.
[69] F. Rosso, A. Giordano, M. Barbarisi, A. Barbarisi, *J. Cell. Physiol.* **2004**, *199*, 174 – 180.
[70] J. Löfberg, K. Ahlfors, C. Fällström, *Dev. Biol.* **1980**, *75*, 148 – 167.
[71] L. S. Campos, *BioEssays* **2005**, *27*, 698 – 707.
[72] A. B. Prowse, F. Chong, P. P. Gray, T. P. Munro, *Stem Cell Res.* **2011**, *6*, 1 – 12.
[73] E. Förster, A. Tielsch, B. Saum, K. H. Weiss, C. Johanssen, D. Graus-Porta, U. Müller, M. Frotscher, *Proc. Natl. Acad. Sci. USA* **2002**, *99*, 13178 – 13183.
[74] K. Kulangara, K. W. Leong, *Soft Matter* **2009**, *5*, 4072 – 4076.
[75] B. Salhia, F. Rutten, M. Nakada, C. Beaudry, M. Berens, A. Kwan, J. T. Rutka, *Cancer Res.* **2005**, *65*, 8792 – 8800.
[76] H. Bielen, C. Houart, *Dev. Neurobiol.* **2014**, *74*, 772 – 780.
[77] L. Varela-Nallar, N. C. Inestrosa, *Front Cell Neurosci.* **2013**, *7*, 100.
[78] Y. P. Kong, C. H. Tu, P. J. Donovan, A. F. Yee, *Acta Biomater.* **2013**, *9*, 6369 – 6380.
[79] W. Chen, L. G. Villa-Diaz, Y. Sun, S. Weng, J. K. Kim, R. H. Lam, L. Han, R. Fan, P. H. Krebsbach, J. Fu, *ACS Nano* **2012**, *6*, 4094 – 4103.

Manuscript received: October 28, 2017
Revised manuscript received: December 19, 2017
Accepted manuscript online: ■■ ■■, 0000
Version of record online: ■■ ■■, 0000

Neural stem cells (NSCs) are self-renewing cells that generate the major cell types of the central nervous system. The authors review the use of artificial micro- and nano-topographical features to control the orientation of NSCs and their differentiation into neuronal and/or neuroglial lineages. ■■OK? ■■

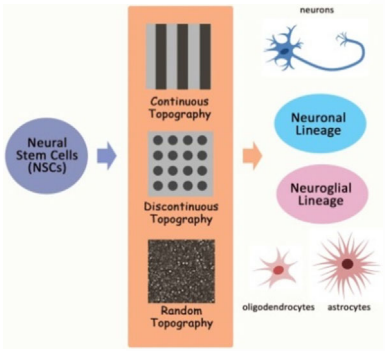

C. Simitzi, K. Karali, A. Ranella, E. Stratakis**

■■ – ■■

Controlling the Outgrowth and Functions of Neural Stem Cells: The Effect of Surface Topography

Controlling the outgrowth and functions of neural stem cells: The effect of surface topography, Simitzi, Stratakis et al. SPACE RESERVED FOR IMAGE AND LINK

Share your work on social media! *ChemPhysChem* has added Twitter as a means to promote your article. Twitter is an online microblogging service that enables its users to send and read short messages and media, known as tweets. Please check the pre-written tweet in the galley proofs for accuracy. If you, your team, or institution have a Twitter account, please include its handle @username. Please use hashtags only for the most important keywords, such as #catalysis, #nanoparticles, or #proteindesign. The ToC picture and a link to your article will be added automatically, so the **tweet text must not exceed 250 characters**. This tweet will be posted on the journal's Twitter account (follow us @ChemPhysChem) upon publication of your article in its final (possibly unpaginated) form. We recommend you to re-tweet it to alert more researchers about your publication, or to point it out to your institution's social media team.

Please check that the ORCID identifiers listed below are correct. We encourage all authors to provide an ORCID identifier for each coauthor. ORCID is a registry that provides researchers with a unique digital identifier. Some funding agencies recommend or even require the inclusion of ORCID IDs in all published articles, and authors should consult their funding agency guidelines for details. Registration is easy and free; for further information, see http://orcid.org/.

C. Simitzi
K. Karali
A. Ranella
E. Stratakis http://orcid.org/0000-0002-1908-8618